isvr Institute of Sound and Vibration Research

A Boundary Element Model for Two-dimensional Elastodynamics on a Single Open or Closed Domain

C.J.C. Jones and D.J. Thompson

ISVR Technical Memorandum 838

May 1999

University of Southampton

SCIENTIFIC PUBLICATIONS BY THE ISVR

Technical Reports are published to promote timely dissemination of research results by ISVR personnel. This medium permits more detailed presentation than is usually acceptable for scientific journals. Responsibility for both the content and any opinions expressed rests entirely with the author(s).

Technical Memoranda are produced to enable the early or preliminary release of information by ISVR personnel where such release is deemed to the appropriate. Information contained in these memoranda may be incomplete, or form part of a continuing programme; this should be borne in mind when using or quoting from these documents.

Contract Reports are produced to record the results of scientific work carried out for sponsors, under contract. The ISVR treats these reports as confidential to sponsors and does not make them available for general circulation. Individual sponsors may, however, authorize subsequent release of the material.

UNIVERSITY OF SOUTHAMPTON

INSTITUTE OF SOUND AND VIBRATION RESEARCH

DYNAMICS GROUP

A Boundary Element Model for Two-dimensional Elastodynamics on a Single Open or Closed Domain

by

C.J.C. Jones and D.J. Thompson

ISVR Technical Memorandum No. 838

May 1999

Authorized for issue by
Dr. M.J. Brennan
Group Chairman

SUMMARY

A Boundary Element model for vibration propagation in two-dimensions has been produced. This has special provision for open boundaries so that the infinite surface of the ground can be modelled as an open boundary of finite length. The effects near to the termination of the boundary are investigated. This report provides an outline theoretical description of the model and instructions for preparing input data and running the program. It also presents a number of example analyses which include a half-space, a thin soil layer and vibration from a tunnel. The model uses three-noded quadratic elements so that the frequency range up to 250 Hz, associated with structure-borne noise from railways, can be covered using a reasonable number of elements. In the case of tunnel vibration, the model indicates that the vibration of the ground surface above th tunnel may be strongly influenced by the tunnel structure. It is important in therefore that in furture work the tunnel structure should be accounted for in the model.

CONTENTS

1. INTRODUCTION

Trains running on lines on the ground surface produce vibration with predominant frequencies between about 4 Hz and 50 Hz. The Boundary Element Method (BEM) has been used previously to model the transmission of vibration in this frequency range [1, 2]. The BEM is advantageous compared with other techniques because it is able to cope with geometrical features such as ditches, embankments and cuttings while also modelling an infinite domain so that a regime of wave propagation is modelled.

The present work is concerned with higher frequency vibration from trains that gives rise to structure borne or 'groundborne' noise. This phenomenon is especially associated with trains running in cut-and-cover or bored tunnels although it has also been associated with trains running on surface tracks [3, 4]. Groundborne noise has dominant frequency components from about 30 Hz to as much as 250 Hz. The need for theoretical models for vibration from tunnels and their role alongside empirical prediction methods is discussed in reference [4]. The objectives in the present development of theoretical models therefore includes the modelling of tunnels and cuttings and the capability, with resonable computing resources, to model waves at 250 Hz.

This report describes a computer program implementing a two-dimensional boundary element (BE) model for elastodynamics. The program is written in Fortran and called GBED4 (Generalised Boundary Element Domain). Although the program has been developed specifically for application to the analysis of vibration propagation from railways it is more generally applicable. The program models a single material domain which may be either finite, with a closed boundary, or infinite, i.e. representing propagation of vibration away from the structure.

In the BEM, the surface of the ground, or structure, is discretized using a set of elements similar to the those of the finite element (FE) method. The program has been developed using the boundary element approach set out in Reference [5]. Since only the boundary is discretized, line elements are used for the two-dimensional case. In the software only a single element type is implemented having three-nodes and quadratic interpolation of the state variables along its length. This represents a higher order element than has been used in the previous work [1, 2] with the aim that it should be suitable for obtaining solutions to the higher frequency required.

A number of example analyses are presented in Section 4 of this report in order to demonstrate the use of the model to cover the frequency range up to 250 Hz and to show the issues that the user must address in constructing a suitable boundary mesh. The cases examined are a homogeneous half-space, a thin ground layer constrained at its lower surface, and vibration from a track foundation in a tunnel set in a homogeneous half-space. For the half-space and layer cases the results of the model are compared with a semi-analytical model [6].

2. THEORETICAL ASPECTS

2.1 Outline of theory

Consider a body Ω with a surface Γ (Figure 1.) The displacement at a point i on the body, in a direction along the direction defined by the basis vector x_l, is denoted by u_l^i.

If time-harmonic solutions are assumed, *i.e.* seeking a formulation for the frequency domain, the integral equation for elastodynamics can be stated as

$$u_l^i + \int_\Gamma \sum_k p_{lk}^* u_k \, d\Gamma = \int_\Gamma \sum_k u_{lk}^* p_k \, d\Gamma \qquad (1)$$

where u_k is the displacement at a point on the surface Γ in the direction of the basis vector k and p_k is a load at a point on the surface Γ in the k direction. The tensor p^*_{lk} represents the solution for the load in the l direction at the interior point i arising from a unit applied displacement at a surface point in the direction k. Likewise, u^*_{lk} represents the solution for the displacement in the l direction at i due to a unit load at the point on the boundary in the k direction. These are known as the Green's function solutions. In performing the integration, the surface point is "moved" around Γ. For the two-dimensional case, the unit solutions p^*_{lk} and u^*_{lk} are 2 by 2 tensors (indicated by the subsrcipts each taking two basis vector directions). The elements of these tensors are functions of the distance between the surface point and the point i. The integral equation, as stated here in terms only of integrals over the surface, assumes that all loads are applied on the boundary and none are applied within the volume of Ω.

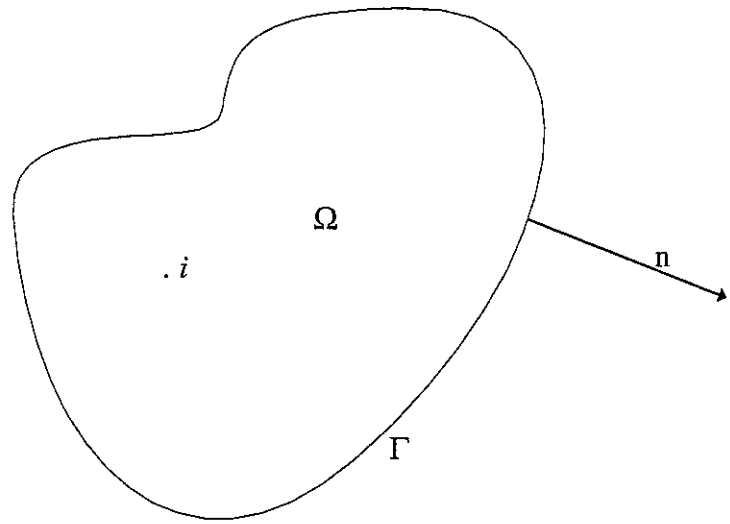

Figure 1. The domain Ω with surface Γ.

The integral equation for the elastodynamic wave field, equation (1), is similar in form to the Kirchhoff-Helmholz integral equation that represents an acoustic wave field and that can be derived from the scalar wave equation. Similarly the integral equation for elastodynamics can be derived from the Navier's differential equations [5]. The Navier's equations for elastodynamics are

$$\begin{aligned}(\lambda+\mu)\frac{\partial\Delta}{\partial x}+\mu\nabla^2 u &= \rho\frac{\partial^2 u}{\partial t^2}\\ (\lambda+\mu)\frac{\partial\Delta}{\partial y}+\mu\nabla^2 v &= \rho\frac{\partial^2 v}{\partial t^2}\\ (\lambda+\mu)\frac{\partial\Delta}{\partial z}+\mu\nabla^2 w &= \rho\frac{\partial^2 w}{\partial t^2}\end{aligned} \qquad (2)$$

where u, v, w are the x, y, z components of displacement $\underline{u}$, $\Delta=\frac{\partial u}{\partial x}+\frac{\partial v}{\partial y}+\frac{\partial w}{\partial z}$ and

$$\lambda=\frac{\sigma E(1+i\eta\,\mathrm{sgn}(\omega))}{(1+\sigma)(1-2\sigma)}, \qquad \mu=\frac{E(1+i\eta\,\mathrm{sgn}(\omega))}{2(1+\sigma)};$$

ω is the circular frequency, E is the Young's modulus, σ is the Poisson's ratio and η is the loss factor representing the material damping of the body.

The Green's function tensors u^*_{lk} and p^*_{lk} for the two-dimensional case are

$$u^*_{lk} = \frac{1}{2\pi\rho {c_2}^2}[\psi\delta_{lk} - \chi\frac{\partial r}{\partial x_l}\frac{\partial r}{\partial x_k}] \tag{3}$$

and

$$p^*_{lk} = \frac{1}{2\pi}\left[\left(\frac{d\psi}{dr}-\frac{1}{r}\chi\right)\left(\delta_{lk}\frac{\partial r}{\partial n}+\frac{\partial r}{\partial x_k}n_l\right)-\frac{2}{r}\chi\left(n_k\frac{\partial r}{\partial x_l}-2\frac{\partial r}{\partial x_l}\frac{\partial r}{\partial x_k}\frac{\partial r}{\partial n}\right)\right.$$
$$\left.-2\frac{d\chi}{dr}\frac{\partial r}{\partial x_l}\frac{\partial r}{\partial x_k}\frac{\partial r}{\partial n}+\left(\frac{{c_1}^2}{{c_2}^2}-2\right)\left(\frac{d\psi}{dr}-\frac{d\chi}{dr}-\frac{1}{r}\chi\right)\frac{\partial r}{\partial x_l}\frac{\partial r}{\partial x_k}\right] \tag{4}$$

where c_1 is the velocity of dilatational waves (P-waves) and c_2 is the shear (S-wave) velocity in the solid. These are calculated from the density ρ, and the Lamé constants λ and μ as

$${c_1}^2 = \frac{\lambda+2\mu}{\rho} \quad {c_2}^2 = \frac{\mu}{\rho} \tag{5}$$

δ_{lk} is the Kroneker delta function, **n** is the unit external normal vector at the surface (with components n_k and n_l) and r is the distance between the source and observation points. The terms ψ and χ are given by

$$\psi = K_o(k_2 r) + \frac{1}{k_2 r}\left[K_1(k_2 r) - \frac{c_2}{c_1}K_1(k_1 r)\right] \tag{6}$$

and

$$\chi = K_2(k_2 r) - \frac{c_2}{c_1}K_2(k_1 r) \tag{7}$$

in which k_1 and k_2 are the dilatational wave number and shear wave number, respectively, K_0, K_1, K_2 are modified Bessel functions of the second kind and of zero, first and second order.

2.2 Discretization

Following general development of the BEM, the next step is to take the point i to the surface Γ. This leads to

$$\varepsilon^i\begin{Bmatrix} {u_x}^i \\ {u_y}^i \end{Bmatrix} + \int_\Gamma \sum_k p^*_{lk}\, u_k d\Gamma = \int_\Gamma \sum_k u^*_{lk}\, p_k d\Gamma \tag{8}$$

where $\varepsilon^i = \begin{bmatrix} \frac{1}{2} & 0 \\ 0 & \frac{1}{2} \end{bmatrix}$ when the boundary at point i is smooth.

Equation (8) is the boundary integral equation to which, as for the acoustic case, the boundary element discretization and collocation method is applied. When the surface point is taken

at the location of the point *i* the Green's function tensors contain infinite terms and this must be dealt with in the integration process.

In the program GBED4 only a single type of boundary element has been implemented; it has three nodes and uses quadratic shape functions. The element is illustrated in Figure 2.

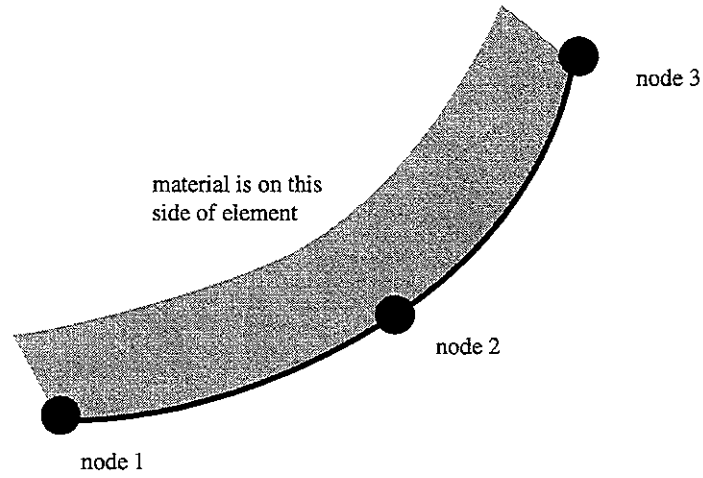

Figure 2. Three-noded, quadratic shape function element.

The process of discretization of the BE formulation uses the finite element approximation method for the functions u and p over the surface as well as to approximate the geometry of the surface from the nodal co-ordinates. For example for the jth element,

$$\mathbf{u} = \begin{Bmatrix} u_x \\ u_y \end{Bmatrix} = \Phi u^j = \begin{bmatrix} \phi_1 & 0 & \phi_2 & 0 & \phi_3 & 0 \\ 0 & \phi_1 & 0 & \phi_2 & 0 & \phi_3 \end{bmatrix} \begin{Bmatrix} u_x^1 \\ u_y^1 \\ u_x^2 \\ u_y^2 \\ u_x^3 \\ u_y^3 \end{Bmatrix} \tag{9}$$

where $\phi_1 = \frac{1}{2}\xi(\xi-1)$, $\phi_2 = (1-\xi^2)$, $\phi_3 = \frac{1}{2}\xi(\xi+1)$ and $-1 \le \xi \le 1$.

For a single point *i*, the discretized boundary equation is

$$\varepsilon^i u^i + \sum_{j=1}^{NE} \left\{ \int_{\Gamma_j} p^* \Phi \, d\Gamma \right\} \mathbf{u}^j = \sum_{j=1}^{NE} \left\{ \int_{\Gamma_j} u^* \Phi \, d\Gamma \right\} \mathbf{p}^j \tag{10}$$

where *NE* is the number of elements and $\mathbf{u}^j$ and $\mathbf{p}^j$ are vectors of nodal values of u and p for the element. u^* and p^* are now 2×6 matrices of terms relating the component directions at the 3 nodes of the element to those at *i*.

For a system of elements with a total of *N* nodes, equation (10) has the form

$$\varepsilon^i u^i + \left[\hat{H}^{i1} \quad \hat{H}^{i2} \quad .. \quad \hat{H}^{iN}\right]\begin{Bmatrix} u_x^1 \\ u_y^1 \\ u_x^2 \\ u_y^2 \\ . \\ . \\ u_x^N \\ u_y^N \end{Bmatrix} = \left[G^{i1} \quad G^{i2} \quad .. \quad G^{iNE}\right]\begin{Bmatrix} \mathbf{p}^1 \\ \mathbf{p}^2 \\ \mathbf{p}^3 \\ . \\ . \\ . \\ \mathbf{p}^{NE} \end{Bmatrix} \tag{11}$$

Notice that here the element matrices, $\hat{H}^{ij}$ are assembled in the finite element sense, i.e. the terms for the nodes common to neighbouring elements are added into the global matrix. The terms of the G matrix however, are not added together but kept separately. This allows the column vector of tractions $\{p\}$ to maintain two separate values at a single node and thus allows the modelling of discontinuous applied tractions at the boundary.

By allowing the point i to take the position of each node in turn, a full set of equations is obtained in the form

$$\underset{(N\times N)}{H}\quad\underset{(N\times 1)}{U} = \underset{(N\times 3\,NE)}{G}\quad\underset{(3\,NE\times 1)}{P} \tag{12}$$

where U and P are the global vectors of nodal displacements and tractions. The definition of H now contains the $\hat{H}^{ij}$ terms and ε^i terms on the diagonal. For the case where the tractions are known at all nodes the multiplication on the right-hand side of equation (12) can be carried out to form the system

$$\underset{(N\times N)}{A}\quad\underset{(N\times 1)}{X} = \underset{(N\times 1)}{B} \tag{13}$$

which is solved for the unknowns X, *i.e.* the nodal displacements. In the case of mixed boundary conditions, columns of equation (12) must be swapped to isolate all the unknowns of the system in X of equation (13). Care must be taken in this process when dealing with the case of two elements of P referring to the same node. Of, course, the solution for the unknown values of P allows only a continuous function of traction at the nodes.

Once the solution has been obtained for the all the values of u and p at all boundary nodes the discretized form of equation (1) can be used to obtain the solution for points inside the domain by using a Gauss-Legendre quadrature to approximate the integrals on all elements.

2.3 Evaluation of singular integral terms

In constructing the global equation (10) the integrals are evaluated for the Green's functions on each element making up the total integration round the boundary. For most of the elements, by using the finite-element type mapping of the element using the shape functions, the integral can be calculated using a suitable Gauss-Legrendre quadrature rule. In the program GBED4 a 10 point rule is used. The high order of this quadrature reflects the high polynomial order of the integrand.

When the collocation node, i, is on the element j the integrand becomes singular for both the evaluation of $\hat{H}$ and G. The singular terms of the G matrix may be integrated using a special quadrature rule that takes into account the presence of a weak singularity which is of logarithmic order. The singularity in the $\hat{H}$ term, however, is of the order $1/r$ and is not integrable. The reason that the total integration round the boundary for these terms has a finite result is that the integrand has opposite signs either side of each node and the singularities cancel. The implication of this is that the diagonal terms of the H matrix cannot be evaluated using any quadrature scheme on an element by element basis.

Following reference [5], for a closed boundary, the difficulty in calculating the diagonal terms of H can be overcome by splitting the evaluation of the H integrand at the Green's function level into two parts, the first part representing the static elasticity case, and the second making up the rest of the value of the Green's function for the dynamic case at the solution frequency. This is achieved by expanding the functions K_0, K_1, K_2 as a series and collecting the terms which correspond to the Green's function for the elastostatics problem [5]. The singular part of the H terms is related only to the static case. The separated-off terms that complete the dynamic terms of H can therefore be evaluated using the standard Gauss-Legendre quadrature.

For the static case, a static rigid body motion, for example represented by a vector U containing one's in all the u_x terms, (or the equivalent in the y direction) must be associated with zero applied loads round the boundary (see equation (10)). This implies that the sum of the row of terms of H for either degree of freedom at each node i must be zero and the diagonal term can be evaluated as.

$$H_s^{ii} = \varepsilon^i + \hat{H}_s^{ii} = -\sum_{nodesj \neq i} \hat{H}_s^{ij} \tag{14}$$

This method evaluates the singular integral term and the value of ε^i simultaneously and is therefore efficient in dealing with the case of node i being at a corner, rather than at a smooth part of the boundary, when $\varepsilon^i \neq 1/2$.

In the present work a method that deals with boundaries which are left open to approximate an infinite boundary such as the ground surface is required. It has already been stated that the singular integral terms of the H matrix cannot be dealt with by integrating element by element. For GBED4, therefore, a preliminary process is carried out whereby each pair of elements is taken in turn and a small closed boundary is constructed by adding a small number of new elements to the pair of elements (Figure 3). It has been found that 5 extra elements are sufficient, making each closed boundary 7 elements (see below).

The terms H_s^{ii} are evaluated using the method implied by equation (14) for the mid-nodes of the two orignal elements and the node in common between them and stored for use in the matrix equation for the full boundary later on. This method is valid since the terms may be seen as dependent only on the integration over the elements to which the node i belongs and is therefore independent of the new 'false' boundary that is set up temporarily. This method is efficient since although setting up the H matrix for NE boundaries of 7 elements is required, this is fast compared to the setting up of the rest of the H for the complete boundary where NE is much larger than 7. The process of determining the terms H_s^{ii} need only be carried out once and the results can be used to set up the global matrices for solutions at all frequencies required thereafter.

In GBED4 it is possible for the construction of the small boundary to fail at a pair of elements for certain geometries where a combination of the three following conditions apply

- contiguous elements differ greatly in length
- an angle close to 2π exists between the two elements
- either of the elements is strongly curved.

Since these conditions would represent very poor practice in discretizing a BE model for a wave propagating problem the conditions where this method produces unacceptable results should not cause a difficulty in practice. In fact the method has been tested and found to be stable and accurate in the evaluation of the singular terms for a variety of possible element geometries. Very little improvement occurs if more than 5 new elements are chosen to complete the closed boundary.

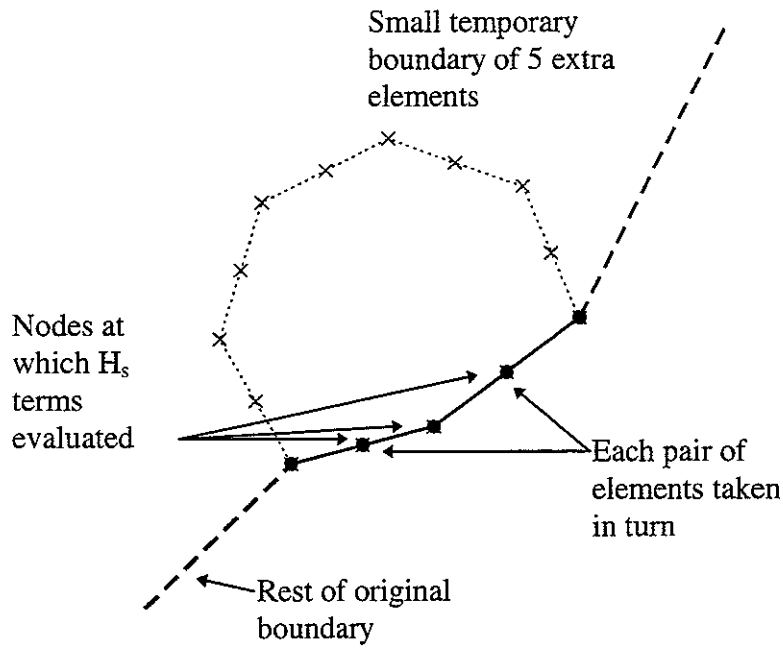

Figure 3. Small boundary constructed around each pair of elements.

Nodes on the 'loose' ends of a boundary, where it has been left open to approximate an infinite boundary have been allotted the value $\varepsilon^i = \begin{bmatrix} \frac{1}{2} & 0 \\ 0 & \frac{1}{2} \end{bmatrix}$ and $\hat{H}_s^{ii} = \mathbf{0}$. This imposes the assumed condition that, at this point, the boundary is smooth and that the elements either side of this node (implied) are straight lines. Since the ends of the boundary should be at a distance from the region where a solution is required, this should cause no difficulty in practice.

3. DATA PREPARATION

When the program is run from a command line the only requests for input are the data and output file names (including path). GBED4 has a single input data file, the structure of which is described in this Section. An example data file is presented in Appendix B. In defining the boundary, consideration should be given to the element size and the extent of the discretization ('mesh') representing an infinite boundary (see Section 2.3 and example analyses). These issues are therefore covered in the discussion of the example analyses.

3.1 General method of data specification

The data is specified in the input text file in *modules* under the following *headers*. A *header* must start with the '*' chacracter but may be in upper or lower case.

**title*

**material*

**frequency*

**nodes*

**elements*

**internal*

**end*

**

After the header, the relevant data must appear in the following lines without blank lines between lines of data. The data modules may be placed in any order and each must appear once in the data file with the exception of the **internal* and **title* modules which are optional, and the ** header which may appear many times or not at all.

The data for each module is described in the following sections 3.2 to 3.9. Numerical data is read line by line with no regard to column position except that it must be contained in the first 132 columns of the line in all cases. A line of numerical data may contain a *comment* after the required number of data items. The start of the comment is indicated by a '!' character. In general the program will check that the required number of numeric data items is found on the line and will halt, giving an error message in the output file, if these are not found.

SI units should be adhered to for input parameters in all data modules.

The maximum number of nodes, elements, frequencies and field points, are set at the time of compiling the program in the include file *be_dim.inc*. This file is listed and other information for compiling the program may be found in Appendix C.

3.2 The **title* module

After the header only one line of data is required. This is a line of up to 132 characters of text which appears in the output file. It is suggested that this input be used to identify analyses, giving date information, a structure name, job reference etc as the user specifies.

3.3 The **material* module

A single data line is required containing the values of Young's modulus, variable name, *E*, the Poisson's ratio, *xnu*, the mass density, *ro*, and loss factor *losf*. This data defines the single domain material.

3.4 The **frequency* module

This module specifies the list of frequencies at which the displacement responses are required. The header is followed by a list of frequencies which should be typed one per line.

3.5 The **nodes* module

The co-ordinates of the boundary nodes are listed in this module. A single line entry containing the x and the y co-ordinate must be made for each and every node of the boundary discretization ('mesh'). These are read into program variables *x(node no.), y(node no.).* No node numbers are specified as these are generated by the program. However, it has been found useful for cross-reference for the user to mark the node numbers after the nodal co-ordinates using the comment facility (see example data file in Appendix 2). No redundant nodes are permitted, i.e. each node must belong to at least one element.

3.6 The **elements* module

This module contains the information both about the element topology and the loading applied to the boundary element domain. The module contains one line of data for each element of the mesh. The element data must name all nodes defined in the *nodes module as being part of at least one element. As is the case for the nodal co-ordinate data, no numbering is specified to the program as this is generated by the program itself. Again it is useful for cross-referencing with node numbers, and hence positioning of applied loads or prescribed displacements, for the user to mark the element numbers in order using the comment facility.

The structure of the data listed for each element is as follows. The data for a single element must occupy only a single line in the data file and must not exceed 132 columns in total.

- the first three numbers on the line are the node numbers of the element which must be in the order shown in Figure 2. These three numbers are therefore interpreted as integers, *betop(element no., 1..3).* Note that the node numbers are allocated by the software according to the order in which their co-ordinates are given in the **node* data module.
- The next two numbers are also interpreted as integers. These are read into the variable *bcode(element no. 1..2)* and indicate the nature of the boundary conditions, given in the rest of the data line, for the x and y directions on the the element respectively. Each integer should be either 0 indicating that the boundary conditions are to be read as prescribed displacement, or 1 indicating that the boundary conditions are to be read as prescribed tractions. For clarity these integers are echoed either as a 'd' or a 't' in the output file. An unrecognised value in this data position (*i.e.* not 0 or 1) is indicated in the output by the letter 'u' although it will not cause the program to fail but will by default be taken as a prescribed traction.

The rest of the data line consists of the prescribed boundary condition values. In general the real and imaginary parts are given for each of the nodes of the element in order, first for the x direction values and then for the y direction values. A full statement of the boundary condition values entails a further 12 floating point number values to be specified. These are read into the complex variables *xbval(element no., 1 .. 3)* and *ybval(element no., 1 .. 3).* In order to reduce the work in specifying the boundary conditions a number of alternative ways of entering this data have been implemented on an element by element basis as follows.

If the number of values found on the element data line is 17 then read the full data as
Re{x value at node 1} Im{x value at node 1}
Re{x value at node 2} Im{x value at node 1}
Re{x value at node 3} Im{x value at node 1}

Re{y value at node 1} Im{y value at node 1}
Re{y value at node 2} Im{y value at node 2}
Re{y value at node 3} Im{y value at node 3}.

If the number of values found is 5
assume all boundary values for the nodes of this element are zero.

If the number of values found is 9 assume all nodes have the same values as
Re{x value at nodes 1, 2 and 3} Im{x value at node 1, 2 and 3}
Re{x value at node 2, 2 and 3} Im{x value at node 1, 2 and 3}.

If the number of values found is 11 assume all imaginary parts are zero and read
Re{x value at node 1}
Re{x value at node 2}
Re{x value at node 3}
Re{y value at node 1}
Re{y value at node 2}
Re{y value at node 3}.

3.7 The **internal* module

The co-ordinates of the *internal nodes* or *field points* are listed in this module. A single line entry containing the x and the y co-ordinate must be made for each field point. As for the boundary nodes, no numbering is specified. Field points should lie within the domain defined by the boundary nodes and elements. (The displacement for a field point outside the domain boundary will be close to zero - the actual value being obtained for such a field point may be taken as an indicator of the accuracy of the discretization.)

3.8 The **end* header

This header signifies the end of the input data and should be placed as the last line of the input data file. There are no data lines associated with this header.

3.9 The ** header

This is a means of including comment lines between other data modules. All text on the rest of a line which starts with ** is ignored by the program. Comments included in this way must not interupt the data in any of the other modules. There are no data lines associated with this header. There may be as many occurences of this header as the user wishes.

3.10 Checking of input data

A Matlab (version 4.2) program, called *beplot.m*, has been written for checking the input data and presenting it graphically. A description of this program is given in Appendix A.

3.11 Results file

A single output file is written by the program. This is a text file which echoes the input parameters and then lists the output at each frequency separately, first for the boundary *nodes* and then for the *field points*. The output is the complex amplitude of displacement at each node/field point location. It is listed in the following columns

- x co-ordinate of node or field point
- y co-ordinate of node or field point
- real part of complex amplitude of displacement in the x direction
- imaginary part of complex amplitude of displacement in the x direction
- real part of complex amplitude of displacement in the y direction
- imaginary part of complex amplitude of displacement in the y direction

Note that, although the output is listed in the order of the node numbers, and field point numbers, used inside the program, no node numbers, or field point numbers, are referenced in the output file.

The output file is easily edited into a form which can then be read into a spreadsheet or "loaded" into Matlab. An ancilliary program, *ex_frf*, is used to extract frequency response functions from the output file at single node or field point locations. This is described in Appendix A.

4. EXAMPLE RESULTS

4.1 Scope of examples

In order to validate the program and to investigate the accuracy of the method a number of examples have been analysed. These demonstrate the capability of the program to model an elastic half-space, a relatively thin soil layer, and vibration propagation from a tunnel. The examples all use a particular set of material properties which are given in Table 1. These represent a relatively soft soil.

Table 1. Material properties for soil.

Young's modulus	157×10^6 Nm^{-2}
Poisson's ratio	0.18
Density	1517 kgm^{-3}
Loss factor	0.1
Compression wave speed	336 ms^{-1}
Shear wave speed	210 ms^{-1}

In order to aid in the discussion of the results the wavelengths of S-waves and P-waves in the medium defined in Table 1 are given in Table 2 at selected frequencies for which example results are presented.

Table 2. P-wave lengths, λ_p, and S-wave lengths, λ_s, in the soil at various frequencies.

	2 Hz	8 Hz	16 Hz	32 Hz	63 Hz	125 Hz	200 Hz	250 Hz
λ_p	168 m	42 m	21 m	10.5 m	5.3 m	2.7 m	1.7 m	1.3 m
λ_s	105 m	26 m	13 m	6.5 m	3.3 m	1.7 m	1.0 m	0.84 m

The analysis examples that are presented in Section 4.2 to 4.4 below have been carried out for a number of frequencies in the range 2 to 250 Hz. For the boundary mesh in each case the length

of each three-noded element has been chosen to be 0.4 m. There are therefore approximately two elements or 5 nodes per wavelength at the highest frequency of the analyses.

4.2 Half-space

A simple elastic half-space is modelled using a line of elements representing the surface of the ground. The idea is that the infinite boundary is approximated by terminating the boundary at x coordinates sufficiently beyond those at which the results are required. In the case generated for the example, the boundary extends from x = -10 m to x = 30 m along the line y = 0 m. The model consists of 100, 0.4 m long, elements and 201 nodes. The input data file for this example is given in Appendix B.

The excitation of the ground under a track structure is modelled as a constant amplitude of vertical stress over a 3.2 m width of the BE surface of the ground centred on x = 0. This represents the vibration contact pressure applied under the ballast layer of a track. The total load is 1 N so that the results represent frequency response functions. No account is taken here of any horizontal component of load at the track.

Results from this BE mesh (and the soil layer example presented in Section 4.3) are directly comparable to those from a two-dimensional semi-analytical model [6]. The semi-analytical model, hereafter refered to as "analytical", has been used to provide a comparison by which the approximation error in the BE approach may be evaluated. It should be noted however that the semi-analytical model does use an adaptive numerical integration process in its calculation that may introduce some calculation error for high frequencies and very low response levels.

Figure 5 presents the amplitude of displacement response in the vertical and lateral directions along the whole length of the boundary at 32 Hz in comparison with the analytical model. The result of the BE calculation can be seen to be highly accurate over most of the boundary but departs for the analytical result near to the end of the boundary. In this case the length inwards from the end of the boundary over which the error is significant is about 1/2 λ_s. The size of the elements is adequately small with respect to the wavelengths at this frequency to ensure that the high rate of change of amplitude, and the large range in variation, with distance especially in the lateral response near x = 0 is accurately modelled.

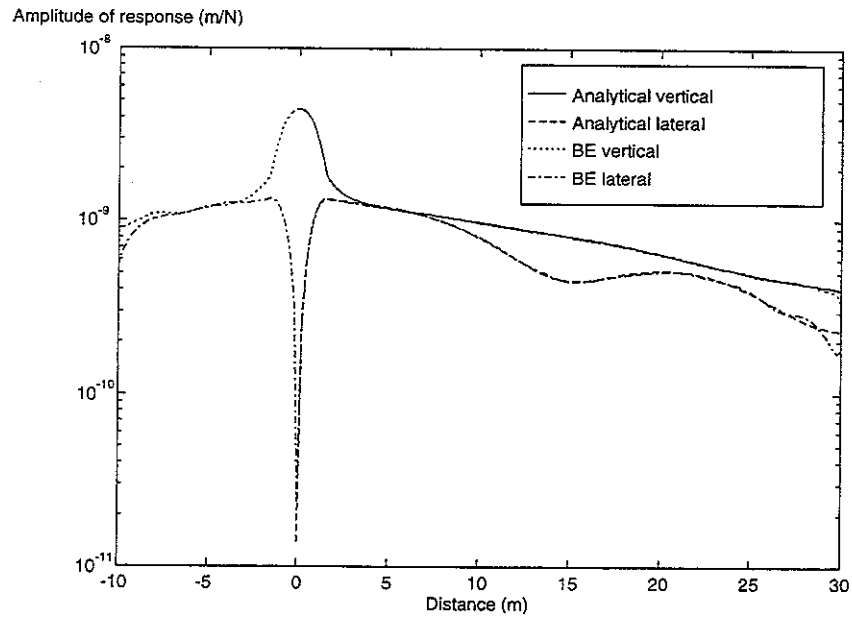

Figure 5 Comparison of response along surface at 32 Hz for the BE model and the semi-analytical model for the half-space.

Figure 6 presents the response across the whole boundary at 63 Hz. It can be seen that the same BE discretization works very well at this frequency and the effect of the boundary termination is confined to an even shorter region in line with the halving of the P-wave and S-wave wavelengths compared to the 32 Hz result of Figure 5.

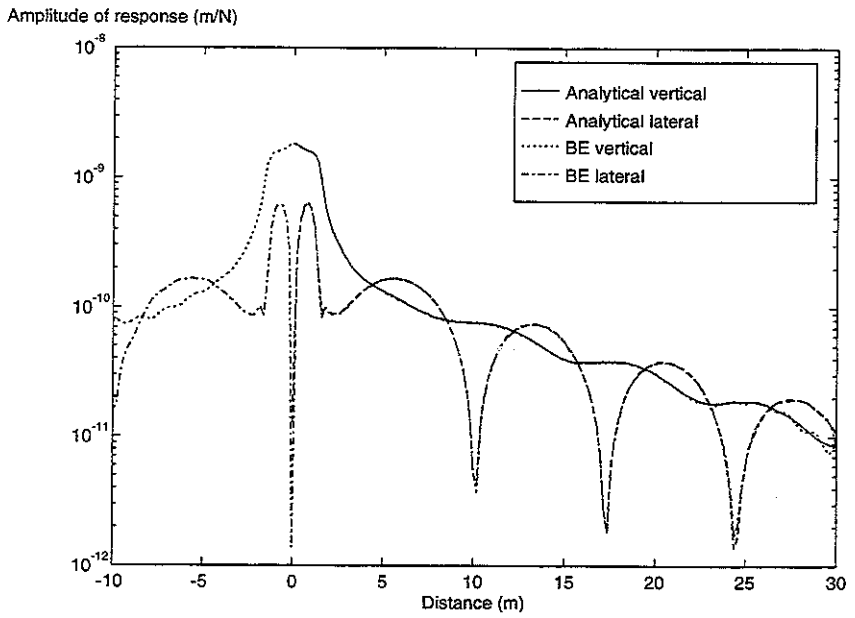

Figure 6 Comparison of response along surface at 63 Hz for the BE model and the semi-analytical model for the half-space.

The results at 125 Hz are presented in Figure 7. At this frequency a general level of error is perceptible as the shear wavelength in the ground is now only about 4 times the element length. Nevertheless, the accuracy is still adequate and the discretization is still able to approximate well

the high rate of change of response ampltiude with distance near the source. The effect of the boundary terminations is difficult to distinguish from the discretization error.

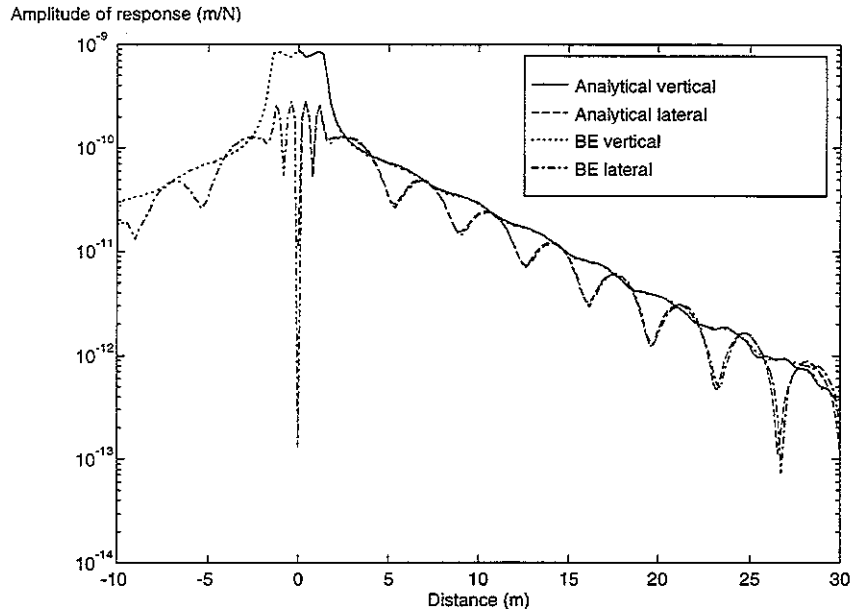

Figure 7 Comparison of response along surface at 125 Hz for the BE model and the semi-analytical model for the half-space.

The results for 200 Hz and 250 Hz are shown in Figures 8 and 9. In these cases the validity of the element size is breaking down and this leads to an increase in the general level of error. This affects the results near the outer right-hand edge of the boundary which are more than 4 decades smaller than the highest levels of response. The fact that this does not occur at the x = -10 m end of the boundary confirms that this is not an effect of the edge of the boundary. Since, in a numerical method such as the BEM, the result at all poisitions along the boundary is obtained by a solution of a single global matrix, the error when viewed, as in these figures, in a relative sense, is high for the very low levels of response further away from the source. Note that in the BEM each degree of freedom of the system is related to every other degree of freedom. This is a result of the integral equation in which the solution for one point on the surface is the integral round the rest of the surface and is reflected in the fact that the matrix is full, *i.e.* all cross-terms between rows and columns are non-zero. The effect is of a "noise floor" which can be seen to exist in the high frequency results, especially at 250 Hz where the element size is such that a wavelength of shear is approximated piecewise by only two quadratic shape function elements.

The comparison of results with the analytical model becomes unreliable as even this is subject to some calculation error for the low response near the outer parts of the boundary in the 250 Hz case.

Attention is now given to the comparison of results for spectra at particular distances along the boundary. Figures 10, 11 and 12 show the response calculated by the BE program compared to the analytical model at 5 m, 10 m and 20 m respectively. The choice has been made therefore not to accept the results near the boundary ends that have already been seen to be subject to some error. From these figures it can be seen that, at these distances, the higher end of the spectrum is modelled well except for the small error, due to element size, near 250 Hz that has already been noted.

The results are not accurate at frequencies below which the extent of the modelled boundary (from left to right) is approximately the same as the wavelengths in the ground. For the 40 m wide boundary this occurs around 8 Hz when λ_p is considered, or 5 Hz if λ_s is considered. In practice, if results in this low frequency range were required, a much longer boundary would be modelled for the same computing cost by using larger elements. Thus to cover a very wide range of frequency two separate BE discretizations may have to be used.

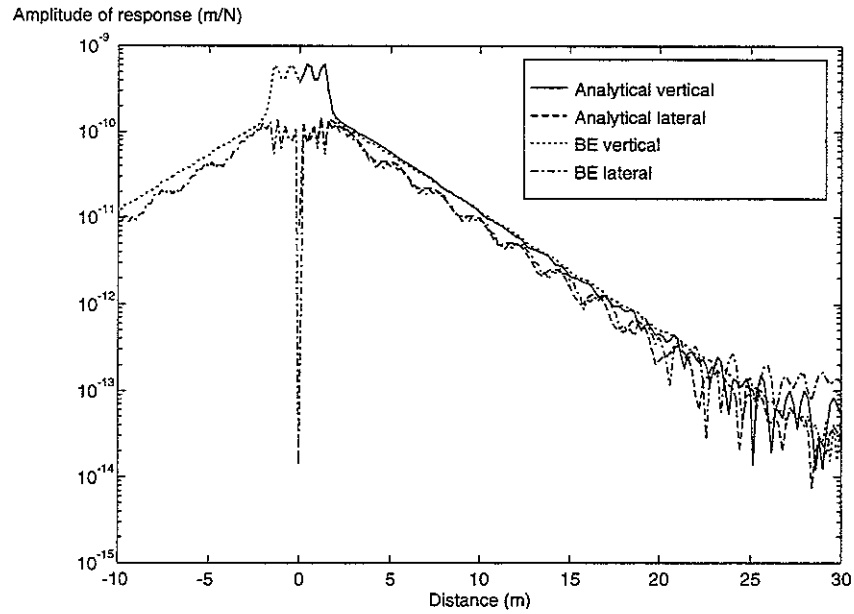

Figure 8 Comparison of response along surface at 200 Hz for the BE model and the semi-analytical model for the half-space.

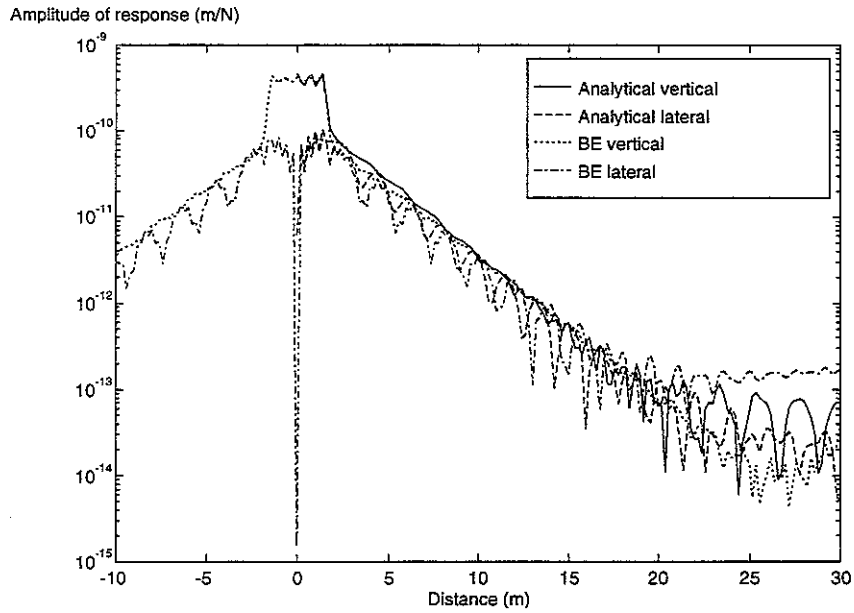

Figure 9 Comparison of response along surface at 250 Hz for the BE model and the semi-analytical model for the half-space.

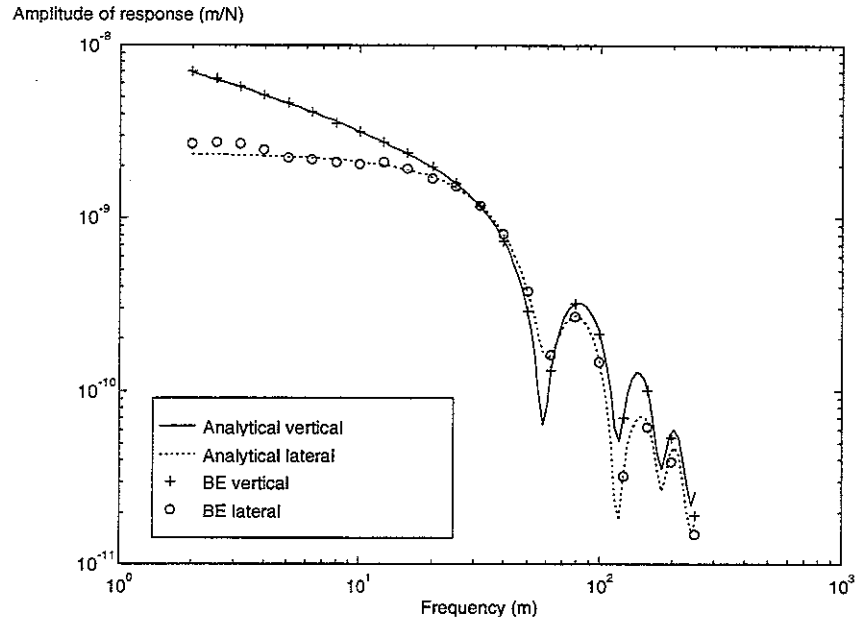

Figure 10 Comparison of frequency response at 5 m for the BE model and the semi-analytical model for the half-space.

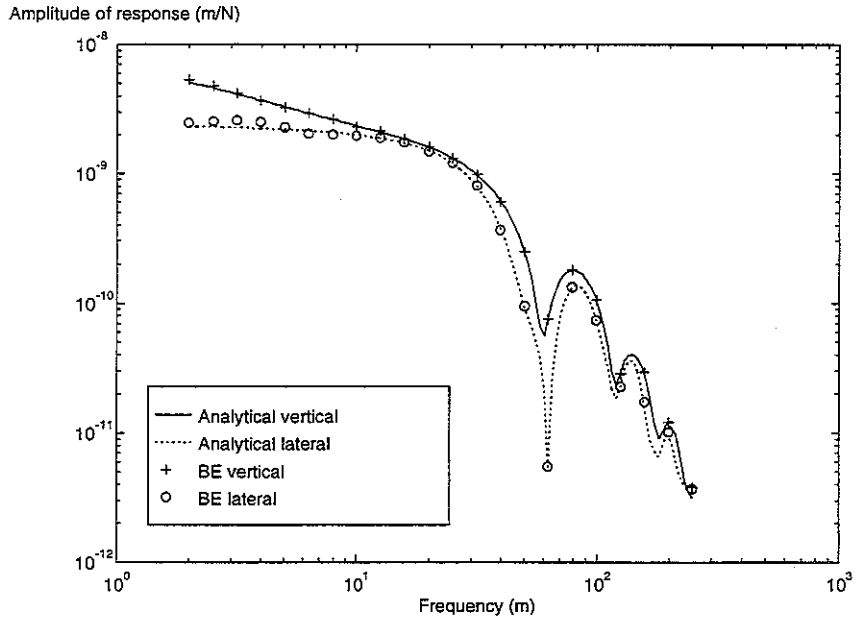

Figure 11 Comparison of frequency response at 10 m for the BE model and the semi-analytical model for the half-space.

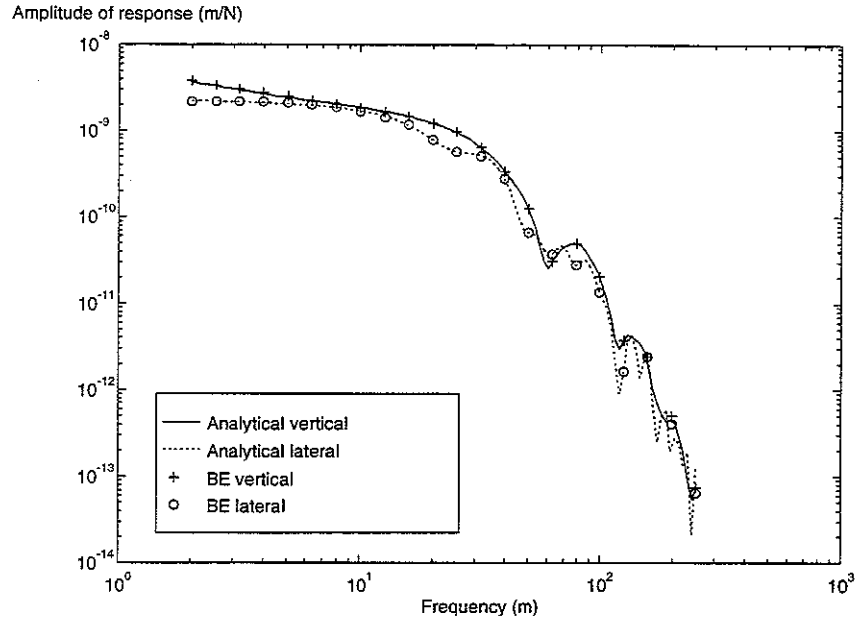

Figure 12 Comparison of frequency response at 20 m for the BE model and the semi-analytical model for the 2 m layer.

In order to visualise wave propagation from a railway, an animated presentation has been prepared using GBED4 with many field points. In the animated sequence, elliptical particle motion can be seen which is typical of a Rayleigh wave, as can wavefronts propagating through the medium away from the source location. Figure 13 shows a still frame from the animation for a frequency of 32 Hz. The shape of the wave front can be seen to develop with distance from the source but at 10 m (only 1 P-wavelength) it has not assumed the shape of a pure Rayleigh wave.

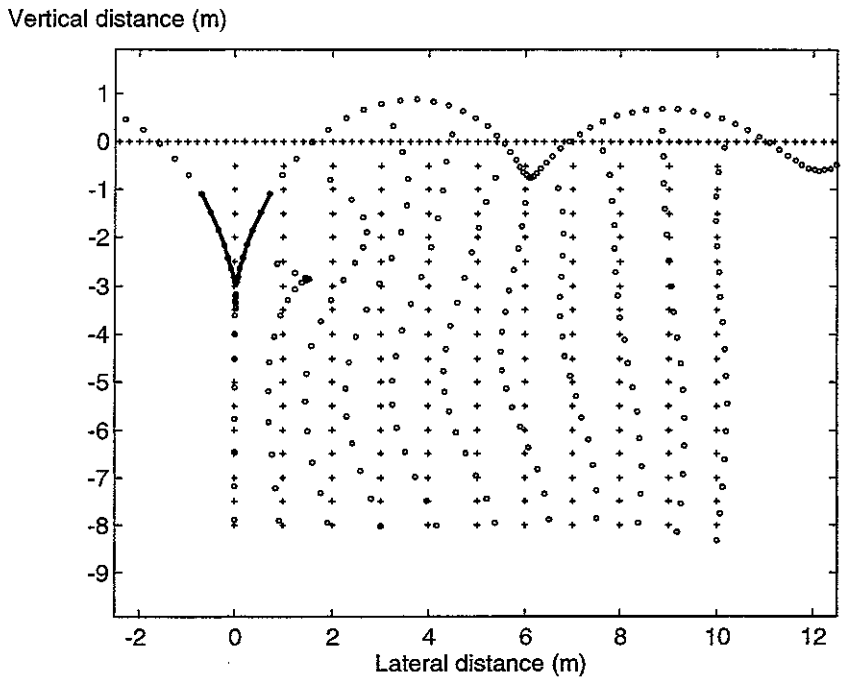

Figure 13. Still picture from animated visualisation of wave propagation in the half-space at 32 Hz; —— location of applied load, o displaced point, + undisplaced point.

Figure 14, from the animated visualisation, shows vibration propagation at 125 Hz. Here it can be seen that, since both λ_p and λ_s are shorter than the width of the source, the propagation has become directional and is 'radiated' downwards into the ground.

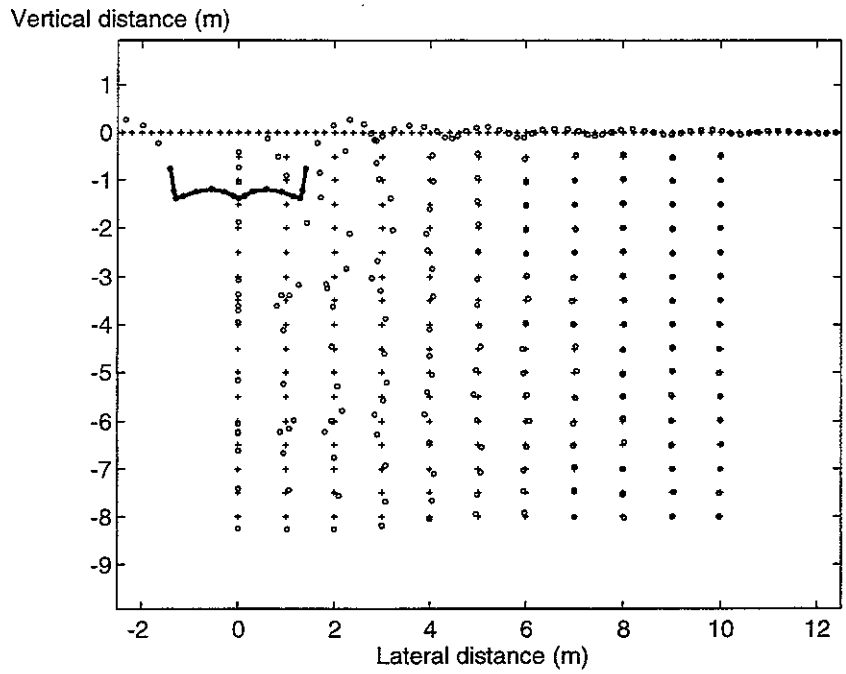

Figure 14. Still picture from animated visualisation of wave propagation in the half-space at 125 Hz; —— location of applied load, o displaced point, + undisplaced point.

4.3 Layer

The example analysis for a 2 m deep layer of soil has been carried out with the same element size. The layer is constrained at its lower boundary as if the layer were resting on a very stiff bedrock.

In modelling a layer using BE, care must be taken to ensure that the separation between surfaces of the model is not small compared to the element length. This would lead to inaccurate quadrature when the collocation node is close to an adjacent boundary for which only the standard quadrature is carried out. However, this is not the case here for the 0.4 m elements used.

In a layered ground, propagation takes place via a number of wave modes and at higher frequencies the variation of the mode shapes with depth is not approximated well by piecewise polynomial approximation methods such as the finite element method. This shows an advantage of the BEM over the FEM since only the function on the boundary is approximated and away from the boundary the Green's functions are used, which take proper account of the oscillation of the solution. Figure 15 presents the dispersion curves for the modes of propagation in the 2 m layer. These have been calculated using the method of Kausel and Roësset [7]. From this it can be seen that to cover the range of frequency up to 250 Hz, it is necessary to model the eighth order PS-V modes. (The decoupled SH modes have only out of plane motion and are not relevant to the two-dimensional model.) Figure 16 shows the mode shapes. At 250 Hz, the first mode ($k = 8.24$ m^{-1} in Figure 16) approximates closely to the Rayleigh wave, that is the only "mode" that exists in a half-space. Other modes up to the eighth mode are highly oscillatory functions of the depth in the layer.

The layer therefore represents a more stringent test of the capability of the BEM to model the mode shapes of propagating waves than does the half-space.

In Figure 15 it can be seen that below about 25 Hz there are no modes of propagation in the layer. This leads to a very strong rate of decay of vibration amplitude with distance at these frequencies and very small response amplitudes away from the load.

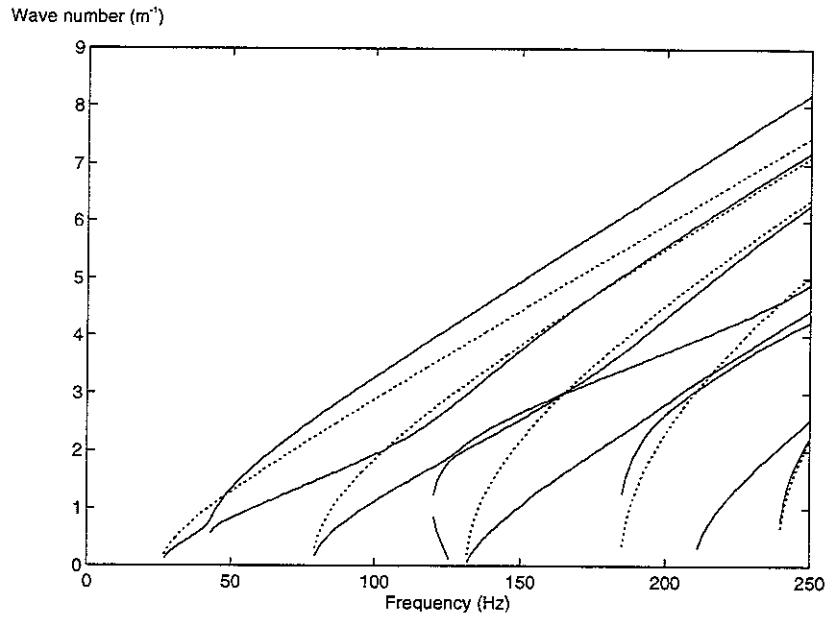

Figure 15. Dispersion curves for the modes of propagation in the 2 m layer;

——P-SV modes, - - - - SH modes.

Figures 17 to 21 show the calculated amplitude of response along the upper surface of the layer at 32 Hz, 63 Hz, 125 Hz, 200 Hz and 250 Hz using both the BEM and the analytical calculation. The effect of the termination of the boundary can be seen to be much stronger in these results than for the half-space. A physical analogy that explains this effect is that a strong change of impedance to wave propagation along the layer is created when the two boundaries forming the layer "open out", compared to the that created at the end of the single boundary in the model approximating the half-space. A stronger reflection of the propagating wave back along the x direction therefore occurs in the model.

Apart from this effect the results are accurate for frequencies up to about 200 Hz where again the general level of error across the whole boundary, that is due to the element size in relation to the propagating wavelength, can once again be seen. The accuracy in this respect is similar to that achieved for the half-space model desipite the variation of amplitude with distance being more complex due to the more complex modal wave propagation regime.

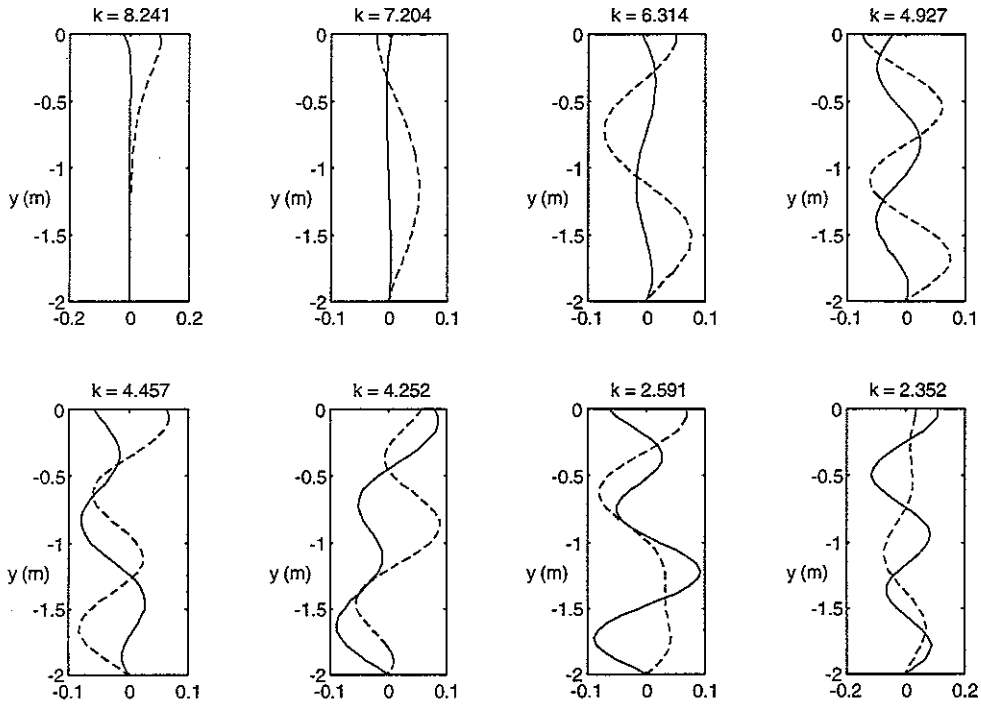

Figure 16. The P-SV mode shapes of the layer at 250 Hz
——— vertical displacement, - - - - lateral displacement.

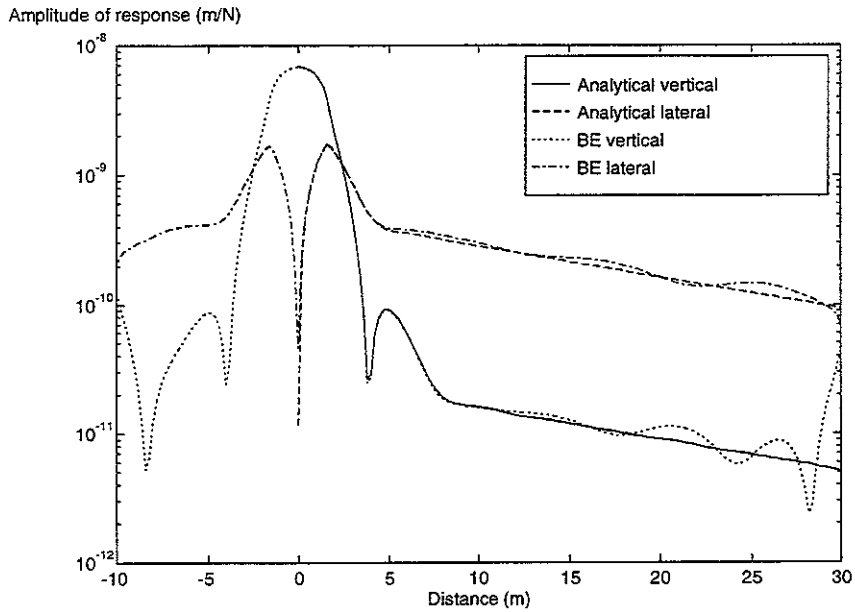

Figure 17. Comparison of response along surface at 32 Hz for the BE model and the semi-analytical model for the 2 m layer.

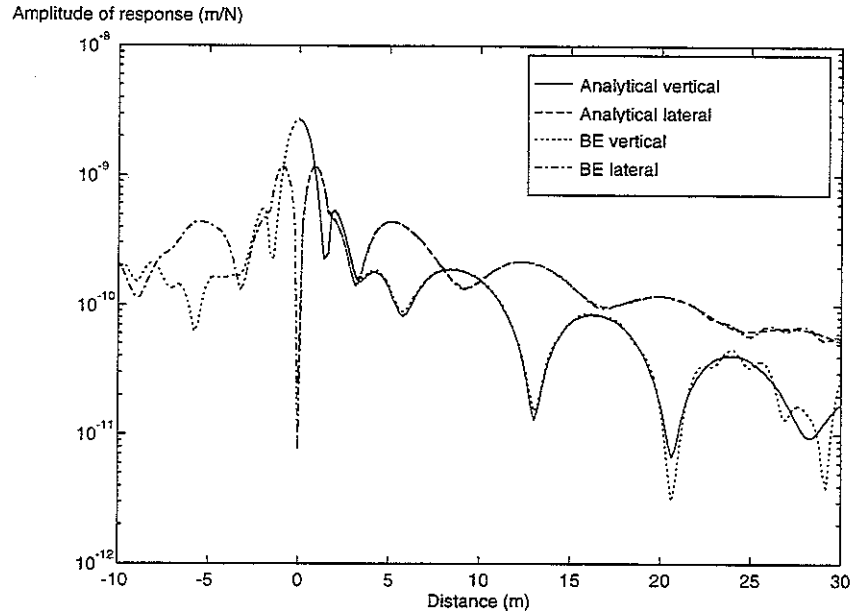

Figure 18. Comparison of response along surface at 63 Hz for the BE model and the semi-analytical model for the 2 m layer.

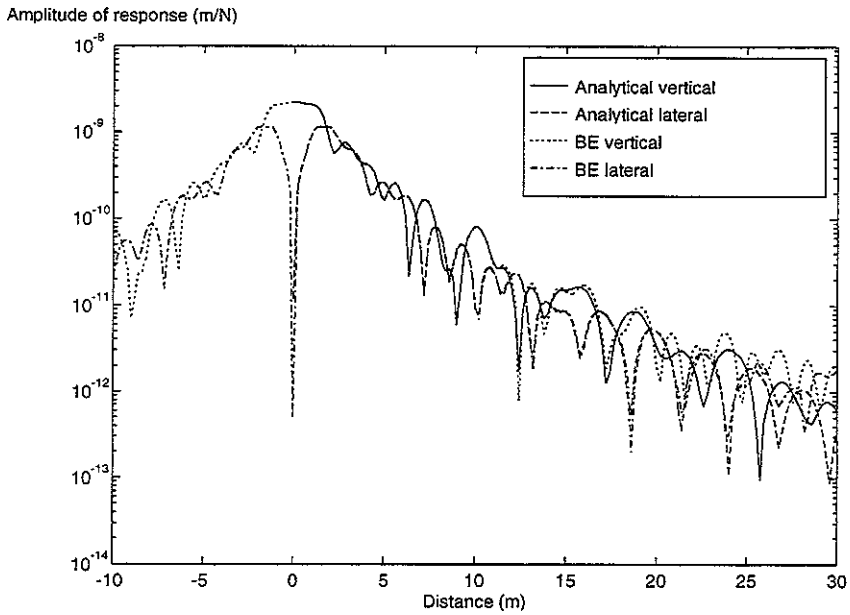

Figure 19. Comparison of response along surface at 125 Hz for the BE model and the semi-analytical model for the 2 m layer.

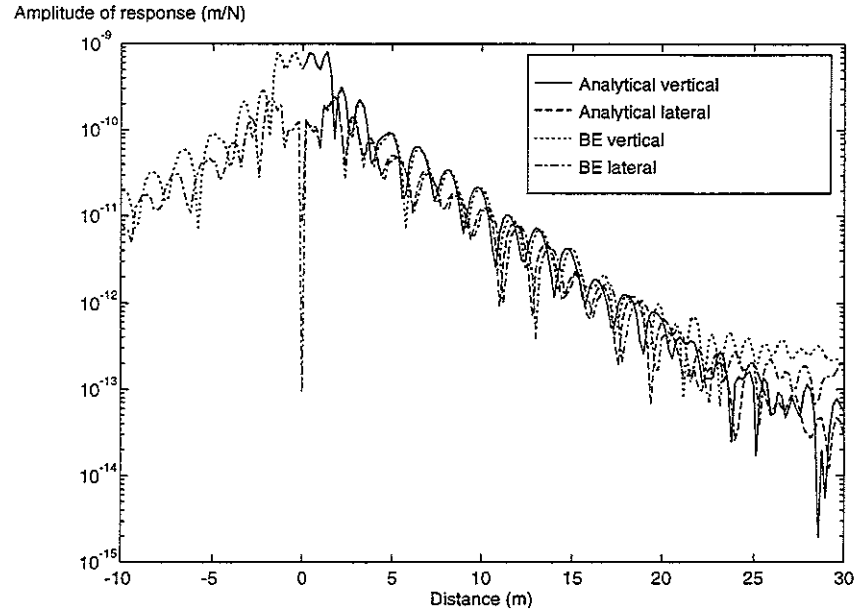

Figure 20. Comparison of response along surface at 200 Hz for the BE model and the semi-analytical model for the 2 m layer.

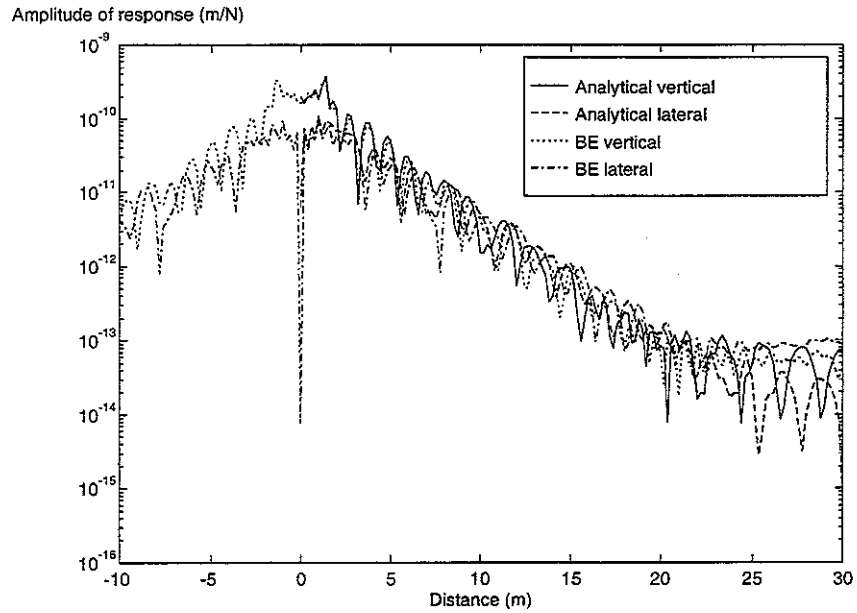

Figure 21. Comparison of response along surface at 250 Hz for the BE model and the semi-analytical model for the 2 m layer.

Figures 22 to 24 show the frequency responses on the layer at $x = 5$, 10 and 20 m. At 5 m the response is acurately modelled over a very wide range of frequency. At low frequency, since there is a rapid decay of vibration along x, because there are no propagating modes, the finite extent of the model compared to the fundamental wave lengths λ_p and λ_s does not lead to a significant error. At 10 m and 20 m the response at low frequency is very small and therefore subject to relative error. The amplitude calculated by the BEM at these frequencies lower than that from the analytical calculation.

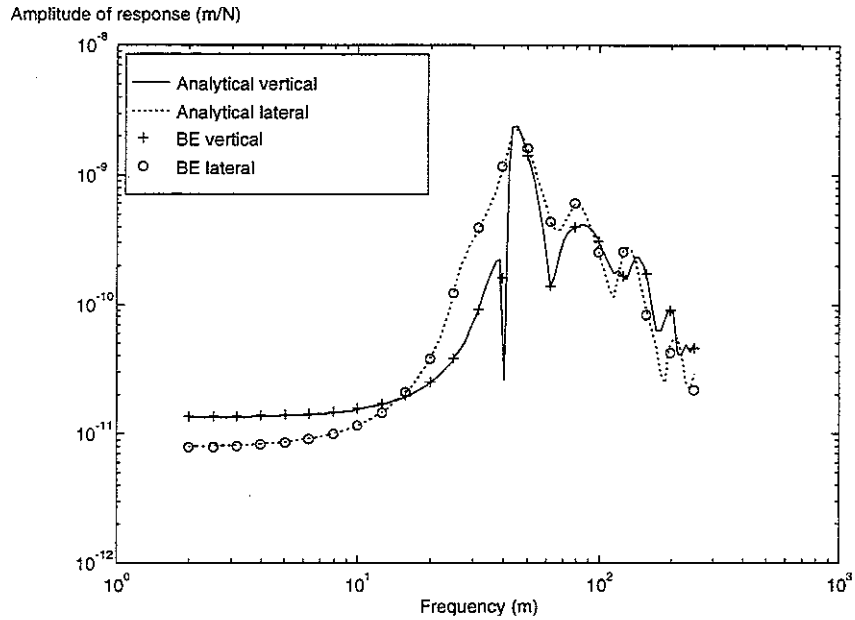

Figure 22 Comparison of frequency response at 5 m for the BE model and the semi-analytical model for the 2 m layer.

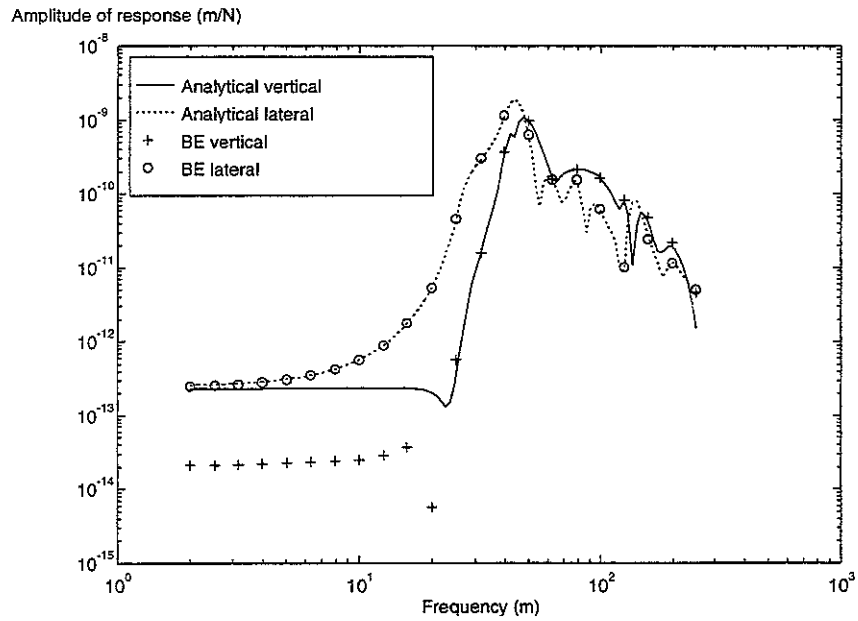

Figure 23 Comparison of frequency response at 10 m for the BE model and the semi-analytical model for the 2 m layer.

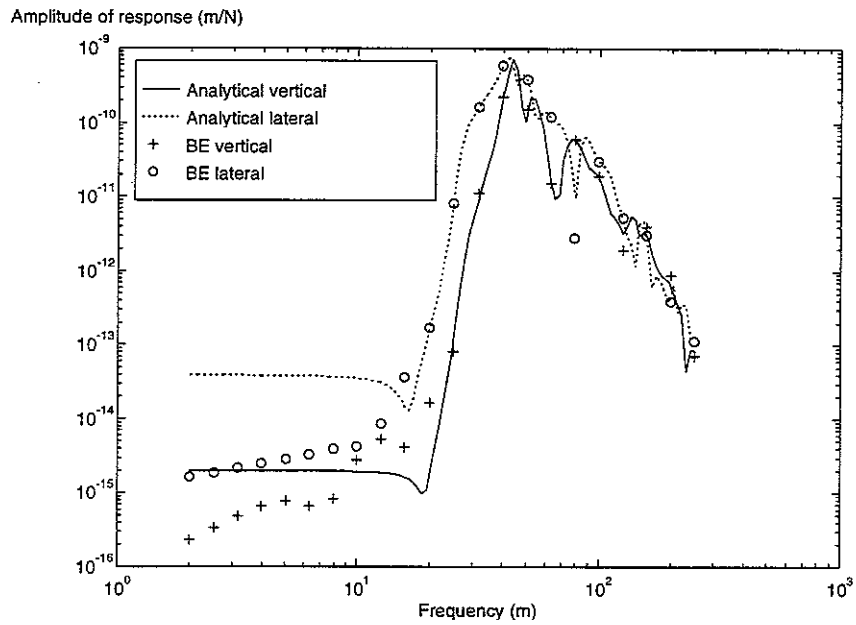

Figure 24 Comparison of frequency response at 20 m for the BE model and the semi-analytical model for the 2 m layer.

4.4 Tunnel

This Section presents some still pictures from an animated visualisation that has been prepared to show the character of vibration propagation from a 3 m radius, bored tunnel. Figure 25 shows the boundary disretization with a unit normal vector at each element pointing inwards towards the domain. In this model the tunnel is represented merely as a circular hole in a homogenous half-space of material. The model contains 198, 0.4 m long, elements. The vertical track load has been applied at the base of the tunnel and has a width of 3.3 m. The ground parameters are still those given in Tables 1 and 2.

Figures 26 to 28 show the response at 8 Hz, 32 Hz and 125 Hz. At 8 Hz the wavelength is large compared to the dimensions of the plot. The tunnel ring is distorted vertically by the applied load. At this frequency the greatest amplitude of response at the ground surface is over the tunnel centre-line.

At 32 Hz (Figure 27) the response of the tunnel ring is modal - the shear wavelength is now appromiately the diameter of the tunnel. At this frequency the highest amplitude is still above the tunnel centre-line. Figure 28, for 125 Hz, shows many wavelengths of vibration around the tunnel ring. In the animated visualisation these can be seen to propagate round the ring and decay towards the crown of the tunnel. At this frequency vibration from the invert of the tunnel is radiated downwards into the ground.

By presenting only the upper half of the field presented in Figure 28, so that the results can be plotted to an expanded scale, Figure 29 shows the vibration propagating upwards towards the ground surface at 125 Hz. It shows that near-circular wavefronts propagate as 'body waves' towards the surface from the upper sides of the tunnel ring. However, the tunnel itself acts as a barrier to wave propagation directly upwards and the highest amplitude of waves is at a distance from the centre-line of the tunnel. The amplitude immediately above the tunnel is controlled by the waves propagating round the tunnel ring. In previous work it has been shown that the vibration response at

the surface within a distance from the tunnel ring approximately equal to the tunnel depth, is controlled by the structural design of the tunnel lining [8].

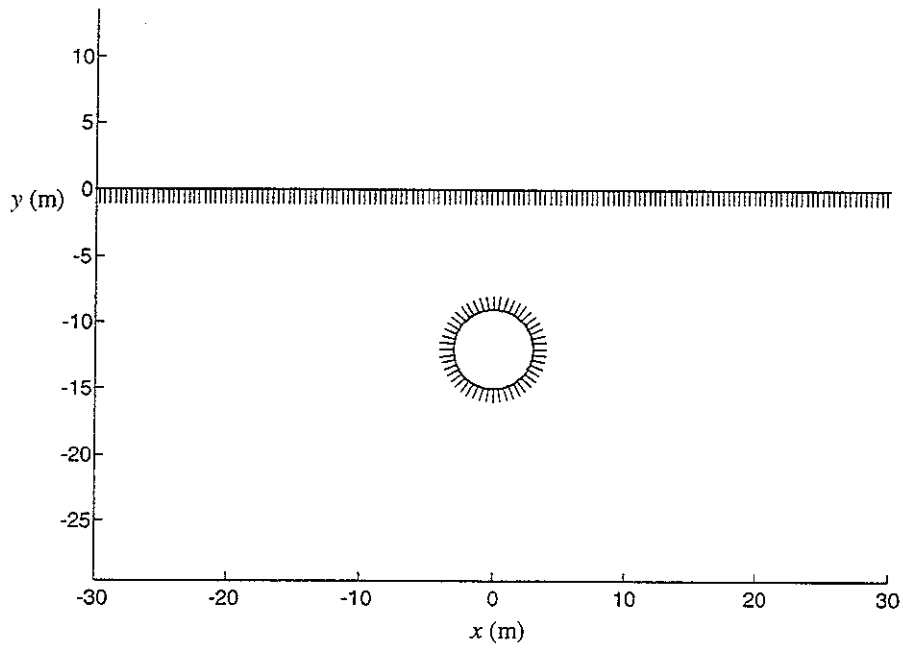

Figure 25. Boundary discretization for the 'tunnel' model.

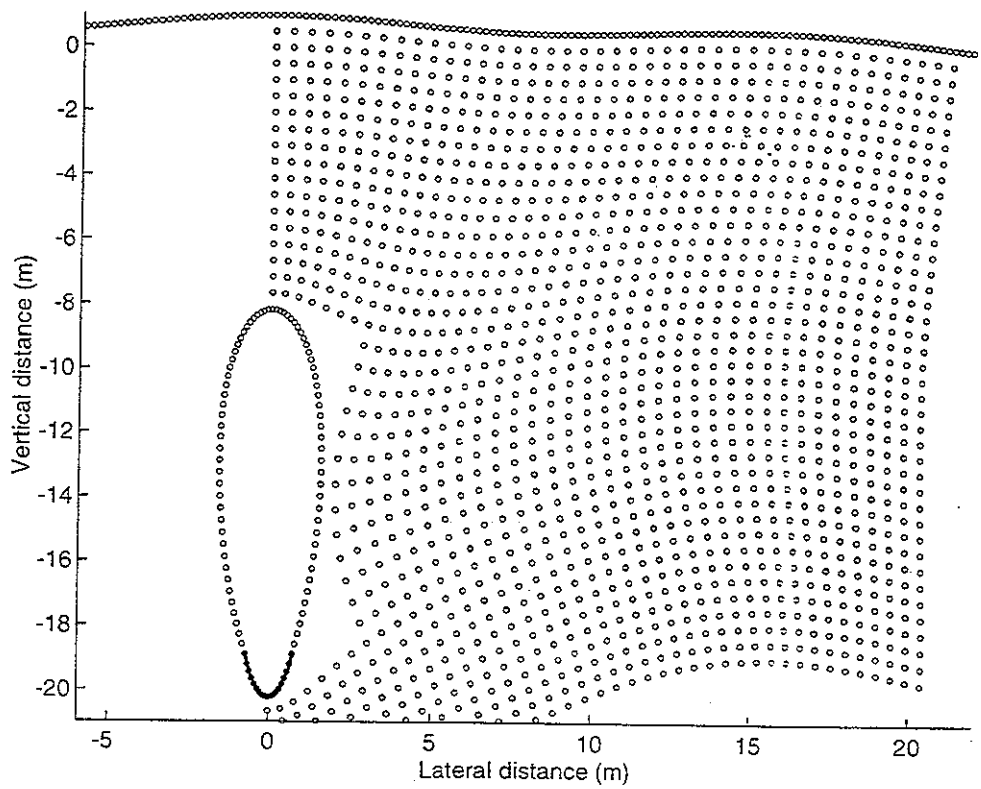

Figure 26 Still picture from animated visualisation of wave propagation from a tunnel at 8 Hz, —— location of applied load, o displaced point.

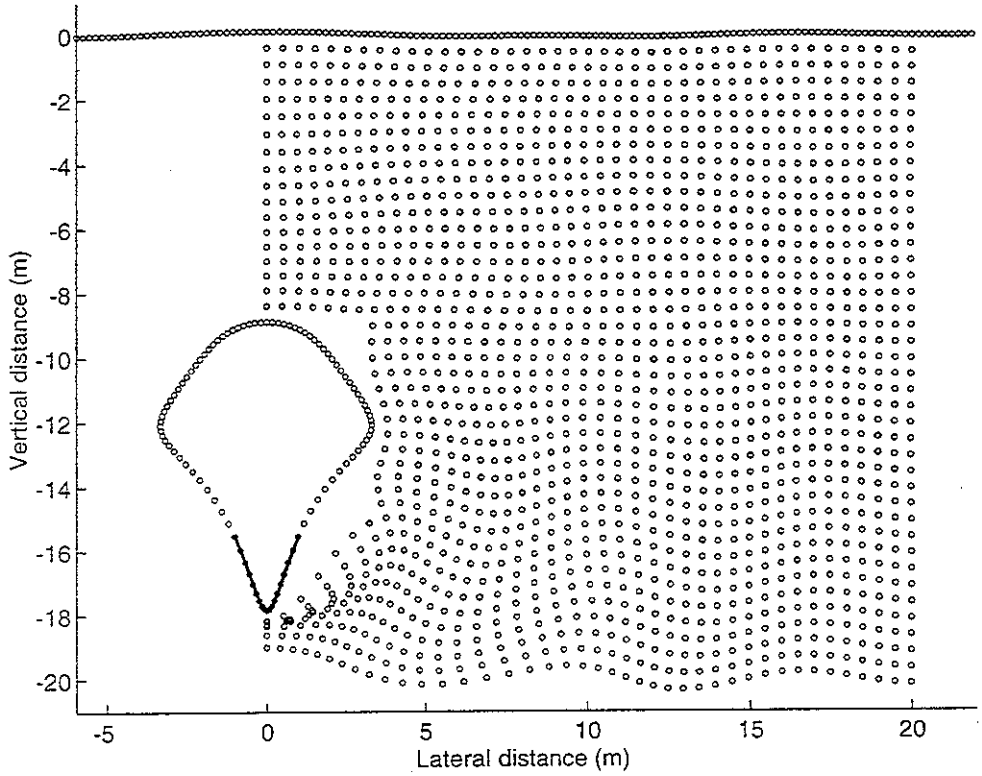

Figure 27 Still picture from animated visualisation of wave propagation from a tunnel at 32 Hz, —— location of applied load, o displaced point.

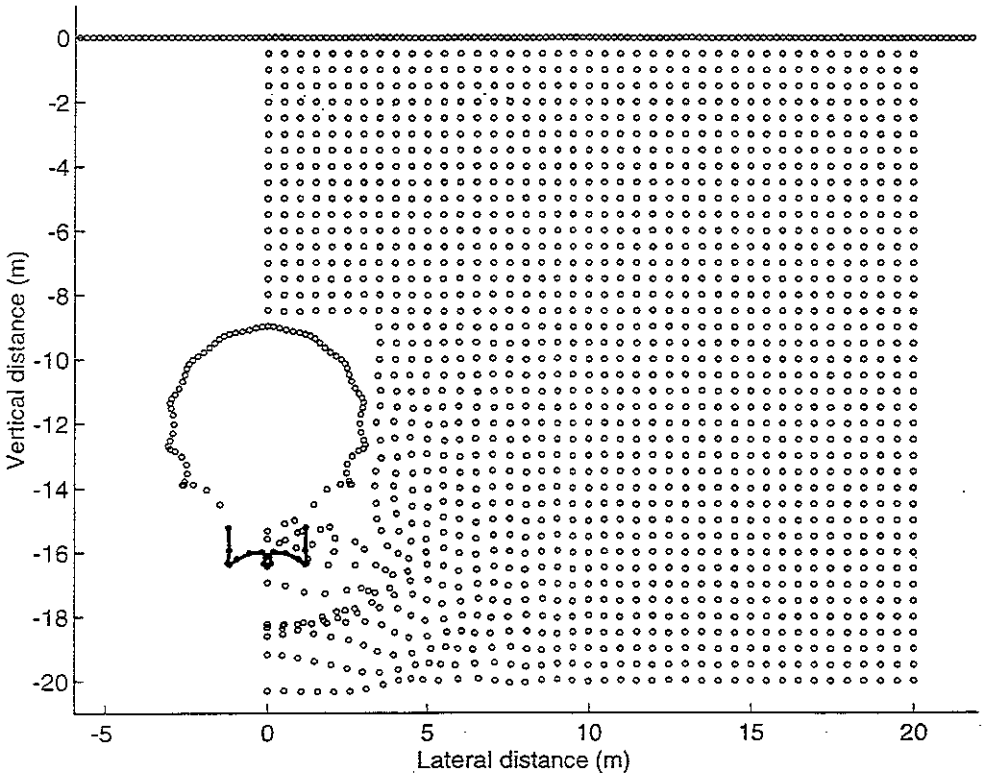

Figure 28 Still picture from animated visualisation of wave propagation from a tunnel at 125 Hz, —— location of applied load, o displaced point.

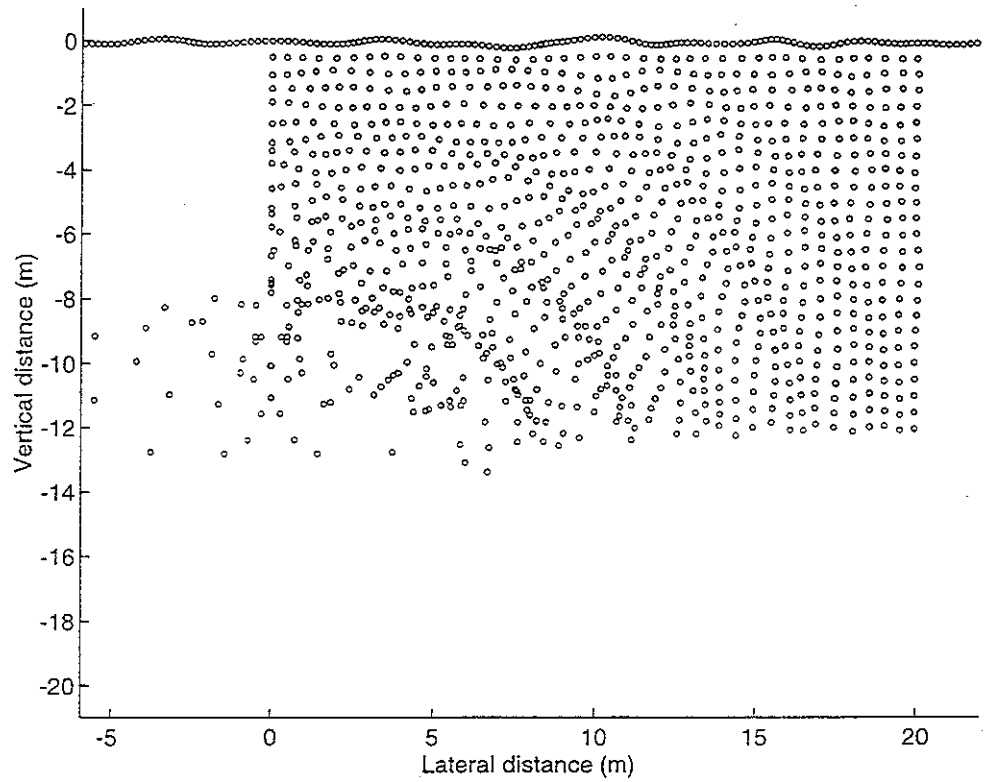

Figure 29 Still picture from animated visualisation of wave propagation from a tunnel at 125 Hz, o *displaced point.*

5. CONCLUSIONS

A program that uses the Boundary Element Method to model the vibration propagation in elastic solids in two-dimensions has been implemented. This uses three-noded quadratic boundary elements and has been shown to be capable of modelling vibration in the range up to 250 Hz with a reasonable number of elements. Special provision has been made for allowing open boundaries so that infinte boundaries, such as the surface of the ground, can be modelled by taking the boundary to a finite distance only. The program can be used to study vibration propagated from the load at the base of a railway track.

When using the model the element size should be chosen so that there are at least about 6 nodes (or two and a half elements) per shear wavelength in the soil for accurate results (corresponding to the 200 Hz results presented). Some error may be expected at locations where the response is more than about 4 decades smaller than the response near the source. Results near to the termination of boundaries are subject to error. The boundary should therefore be extended well beyond the distances at which results are required.

The example analyses have been used to illustrate, by means of an animated presentation, some of effects of propagation in a half-space from a surface source and also from a tunnel source. In this case, the model indicates that the vibration of the ground surface above th tunnel may be strongly influenced by the tunnel structure. It is important in therefore that in furture work the tunnel structure should be accounted for in the model.

6. ACKNOWLEDGEMENT

The work reported has been carried out, and the program described in this report has been developed, under EPSRC grant number GR/L11397.

7. REFERENCES

1. Peplow, A.T., Jones, C.J.C. and Petyt, M 1995 *Proc.Inst.Acoustics*, 17(4), Liverpool, 479 - 486, Ground vibration over uniform and non-uniform layered media: a two-dimensional model.

2. Peplow, A.T., Jones, C.J.C. and Petyt, M 1999 *Applied Acoustics* 56, 283 - 296, Surface vibration propagation over a layered elastic half-space with an inclusion.

3. Jones, C.J.C., 1994 *Proceedings of the Institution of Civil Engineers, Transportation* **105**, 43 - 51. Use of numerical models to determine the effectiveness of anti-vibration systems for railways.

4. Jones, C.J.C., 1996 *Proceedings of Internoise '96,* Liverpool, 421 - 426. Groundborne noise from new railway tunnels.

5. Dominguez, J. 1993 *Computational Mechanics Publications, Southampton (Elsevier Applied Science.)* Boundary elements in dynamics.

6. Jones, D.V. and Petyt, M. 1993 *Journal of Sound and Vibration* **161**, 1-18. Ground vibration in the vicinity of a strip load: an elastic layer on half-space .

7. Kausel, E. and Roësset, J.M. 1981 *Bulletin of the Seismological Society of America* **71**(6), 1743 - 1761. Stiffness matrices for layered soils.

8. Jones,C.J.C., Wang, A. and Dawn, T.M 1995 *Computational Acoustics and its Environmental Applications, Ed. C.A. Brebbia,* Computational Mechanics Publications, Southamtpon, 285 - 292, Modelling the propagation of vibration from railway tunnels.

APPENDIX A - ANCILLARY SOFTWARE

beplot

A Matlab (version 4.2) program, called *beplot.m*, has been written for checking the input data and presenting it graphically. *Beplot* should be run from the Matlab command line.

The Matlab program runs a compiled executable of the Fortran source *gb4chk.for*. This program uses the same input routines (from the same include file) as the main program *gbed4* to read the data and write temporary files for the co-ordinates of the boundary nodes, *xy.tmp*, for the element topology, *betop.tmp*, and for the field point co-ordinates, *fpxy.tmp*. The program *gb4chk* will not normally be run directly by the user. Information for compiling this program is presented in Appendix C.

The temporary files are loaded into Matlab and a number of different graphical representations of the boundary element mesh are obtainable from the menu. These include the boundary nodes (with or without numbering), the elements and the normal to the element which indicates the side of the element on which the material is placed. The Matlab command *zoom*, or the *axes* command, can be used to change the scale of the plot to examine the numbering of individual elements or nodes.

ex_frf

The Fortran program *ex_frf* has been written to simplify the process of plotting data at a single boundary node or field point as a function of frequency. It should be run interactively. It requires the specification of an input file (*i.e.* an output file of the main program), an output file and the x and y co-ordinates of a node or field point at which to extract the frequency dependant response. The output is a text file containing a line for each frequency of the results. There are no column headers in the file and each line contains the following items in order

- frequency
- real part of the amplitude of response in the x direction
- imaginary part of the amplitude of response in the x direction
- real part of the amplitude of response in the y direction
- imaginary part of the amplitude of response in the y direction

The file is suitable for reading into a spreadsheet program or may be read directly into Matlab using the *load* command.

APPENDIX B - EXAMPLE INPUT FILE

In this Appendix an example data file is provided which demonstrates the use of each of the data modules. It corresponds to the example of the half-space for which results are presented in Section 4.2.

```
*title
Half space data file for GBED4 CJCJ 20-4-99
*******************************************
** This file is for the example half-space **
** used to generate results presented in   **
** the Technical Memorandum                **
*******************************************
*material
157.2d6,0.18,1517.0,0.1 ! E, nu, rho, loss factor
*frequency
       32.0
       63.0
     125.0
     200.0
     250.0
*nodes
    30.00000         0.00000 !   1
    29.80000         0.00000 !   2
    29.60000         0.00000 !   3
    29.40000         0.00000 !   4
    29.20000         0.00000 !   5
    29.00000         0.00000 !   6
    28.80000         0.00000 !   7
    28.60000         0.00000 !   8
    28.40000         0.00000 !   9
    28.20000         0.00000 !  10
    28.00000         0.00000 !  11
    27.80000         0.00000 !  12
    27.60000         0.00000 !  13
    27.40000         0.00000 !  14
    27.20000         0.00000 !  15
    27.00000         0.00000 !  16
    26.80000         0.00000 !  17
    26.60000         0.00000 !  18
    26.40000         0.00000 !  19
    26.20000         0.00000 !  20
    26.00000         0.00000 !  21
    25.80000         0.00000 !  22
    25.60000         0.00000 !  23
    25.40000         0.00000 !  24
    25.20000         0.00000 !  25
    25.00000         0.00000 !  26
    24.80000         0.00000 !  27
    24.60000         0.00000 !  28
    24.40000         0.00000 !  29
    24.20000         0.00000 !  30
    24.00000         0.00000 !  31
    23.80000         0.00000 !  32
    23.60000         0.00000 !  33
    23.40000         0.00000 !  34
    23.20000         0.00000 !  35
    23.00000         0.00000 !  36
    22.80000         0.00000 !  37
    22.60000         0.00000 !  38
    22.40000         0.00000 !  39
    22.20000         0.00000 !  40
    22.00000         0.00000 !  41
    21.80000         0.00000 !  42
    21.60000         0.00000 !  43
    21.40000         0.00000 !  44
```

```
 21.20000          0.00000 !  45
 21.00000          0.00000 !  46
 20.80000          0.00000 !  47
 20.60000          0.00000 !  48
 20.40000          0.00000 !  49
 20.20000          0.00000 !  50
 20.00000          0.00000 !  51
 19.80000          0.00000 !  52
 19.60000          0.00000 !  53
 19.40000          0.00000 !  54
 19.20000          0.00000 !  55
 19.00000          0.00000 !  56
 18.80000          0.00000 !  57
 18.60000          0.00000 !  58
 18.40000          0.00000 !  59
 18.20000          0.00000 !  60
 18.00000          0.00000 !  61
 17.80000          0.00000 !  62
 17.60000          0.00000 !  63
 17.40000          0.00000 !  64
 17.20000          0.00000 !  65
 17.00000          0.00000 !  66
 16.80000          0.00000 !  67
 16.60000          0.00000 !  68
 16.40000          0.00000 !  69
 16.20000          0.00000 !  70
 16.00000          0.00000 !  71
 15.80000          0.00000 !  72
 15.60000          0.00000 !  73
 15.40000          0.00000 !  74
 15.20000          0.00000 !  75
 15.00000          0.00000 !  76
 14.80000          0.00000 !  77
 14.60000          0.00000 !  78
 14.40000          0.00000 !  79
 14.20000          0.00000 !  80
 14.00000          0.00000 !  81
 13.80000          0.00000 !  82
 13.60000          0.00000 !  83
 13.40000          0.00000 !  84
 13.20000          0.00000 !  85
 13.00000          0.00000 !  86
 12.80000          0.00000 !  87
 12.60000          0.00000 !  88
 12.40000          0.00000 !  89
 12.20000          0.00000 !  90
 12.00000          0.00000 !  91
 11.80000          0.00000 !  92
 11.60000          0.00000 !  93
 11.40000          0.00000 !  94
 11.20000          0.00000 !  95
 11.00000          0.00000 !  96
 10.80000          0.00000 !  97
 10.60000          0.00000 !  98
 10.40000          0.00000 !  99
 10.20000          0.00000 ! 100
 10.00000          0.00000 ! 101
  9.80000          0.00000 ! 102
  9.60000          0.00000 ! 103
  9.40000          0.00000 ! 104
  9.20000          0.00000 ! 105
  9.00000          0.00000 ! 106
  8.80000          0.00000 ! 107
  8.60000          0.00000 ! 108
  8.40000          0.00000 ! 109
  8.20000          0.00000 ! 110
  8.00000          0.00000 ! 111
  7.80000          0.00000 ! 112
  7.60000          0.00000 ! 113
```

```
 7.40000         0.00000 ! 114
 7.20000         0.00000 ! 115
 7.00000         0.00000 ! 116
 6.80000         0.00000 ! 117
 6.60000         0.00000 ! 118
 6.40000         0.00000 ! 119
 6.20000         0.00000 ! 120
 6.00000         0.00000 ! 121
 5.80000         0.00000 ! 122
 5.60000         0.00000 ! 123
 5.40000         0.00000 ! 124
 5.20000         0.00000 ! 125
 5.00000         0.00000 ! 126
 4.80000         0.00000 ! 127
 4.60000         0.00000 ! 128
 4.40000         0.00000 ! 129
 4.20000         0.00000 ! 130
 4.00000         0.00000 ! 131
 3.80000         0.00000 ! 132
 3.60000         0.00000 ! 133
 3.40000         0.00000 ! 134
 3.20000         0.00000 ! 135
 3.00000         0.00000 ! 136
 2.80000         0.00000 ! 137
 2.60000         0.00000 ! 138
 2.40000         0.00000 ! 139
 2.20000         0.00000 ! 140
 2.00000         0.00000 ! 141
 1.80000         0.00000 ! 142
 1.60000         0.00000 ! 143
 1.40000         0.00000 ! 144
 1.20000         0.00000 ! 145
 1.00000         0.00000 ! 146
 0.80000         0.00000 ! 147
 0.60000         0.00000 ! 148
 0.40000         0.00000 ! 149
 0.20000         0.00000 ! 150
 0.00000         0.00000 ! 151
-0.20000         0.00000 ! 152
-0.40000         0.00000 ! 153
-0.60000         0.00000 ! 154
-0.80000         0.00000 ! 155
-1.00000         0.00000 ! 156
-1.20000         0.00000 ! 157
-1.40000         0.00000 ! 158
-1.60000         0.00000 ! 159
-1.80000         0.00000 ! 160
-2.00000         0.00000 ! 161
-2.20000         0.00000 ! 162
-2.40000         0.00000 ! 163
-2.60000         0.00000 ! 164
-2.80000         0.00000 ! 165
-3.00000         0.00000 ! 166
-3.20000         0.00000 ! 167
-3.40000         0.00000 ! 168
-3.60000         0.00000 ! 169
-3.80000         0.00000 ! 170
-4.00000         0.00000 ! 171
-4.20000         0.00000 ! 172
-4.40000         0.00000 ! 173
-4.60000         0.00000 ! 174
-4.80000         0.00000 ! 175
-5.00000         0.00000 ! 176
-5.20000         0.00000 ! 177
-5.40000         0.00000 ! 178
-5.60000         0.00000 ! 179
-5.80000         0.00000 ! 180
-6.00000         0.00000 ! 181
-6.20000         0.00000 ! 182
```

```
    -6.40000          0.00000 ! 183
    -6.60000          0.00000 ! 184
    -6.80000          0.00000 ! 185
    -7.00000          0.00000 ! 186
    -7.20000          0.00000 ! 187
    -7.40000          0.00000 ! 188
    -7.60000          0.00000 ! 189
    -7.80000          0.00000 ! 190
    -8.00000          0.00000 ! 191
    -8.20000          0.00000 ! 192
    -8.40000          0.00000 ! 193
    -8.60000          0.00000 ! 194
    -8.80000          0.00000 ! 195
    -9.00000          0.00000 ! 196
    -9.20000          0.00000 ! 197
    -9.40000          0.00000 ! 198
    -9.60000          0.00000 ! 199
    -9.80000          0.00000 ! 200
   -10.00000          0.00000 ! 201
*elements
  1   2   3 1  1 !   1
  3   4   5 1  1 !   2
  5   6   7 1  1 !   3
  7   8   9 1  1 !   4
  9  10  11 1  1 !   5
 11  12  13 1  1 !   6
 13  14  15 1  1 !   7
 15  16  17 1  1 !   8
 17  18  19 1  1 !   9
 19  20  21 1  1 !  10
 21  22  23 1  1 !  11
 23  24  25 1  1 !  12
 25  26  27 1  1 !  13
 27  28  29 1  1 !  14
 29  30  31 1  1 !  15
 31  32  33 1  1 !  16
 33  34  35 1  1 !  17
 35  36  37 1  1 !  18
 37  38  39 1  1 !  19
 39  40  41 1  1 !  20
 41  42  43 1  1 !  21
 43  44  45 1  1 !  22
 45  46  47 1  1 !  23
 47  48  49 1  1 !  24
 49  50  51 1  1 !  25
 51  52  53 1  1 !  26
 53  54  55 1  1 !  27
 55  56  57 1  1 !  28
 57  58  59 1  1 !  29
 59  60  61 1  1 !  30
 61  62  63 1  1 !  31
 63  64  65 1  1 !  32
 65  66  67 1  1 !  33
 67  68  69 1  1 !  34
 69  70  71 1  1 !  35
 71  72  73 1  1 !  36
 73  74  75 1  1 !  37
 75  76  77 1  1 !  38
 77  78  79 1  1 !  39
 79  80  81 1  1 !  40
 81  82  83 1  1 !  41
 83  84  85 1  1 !  42
 85  86  87 1  1 !  43
 87  88  89 1  1 !  44
 89  90  91 1  1 !  45
 91  92  93 1  1 !  46
 93  94  95 1  1 !  47
 95  96  97 1  1 !  48
 97  98  99 1  1 !  49
```

```
 99 100 101 1  1 !  50
101 102 103 1  1 !  51
103 104 105 1  1 !  52
105 106 107 1  1 !  53
107 108 109 1  1 !  54
109 110 111 1  1 !  55
111 112 113 1  1 !  56
113 114 115 1  1 !  57
115 116 117 1  1 !  58
117 118 119 1  1 !  59
119 120 121 1  1 !  60
121 122 123 1  1 !  61
123 124 125 1  1 !  62
125 126 127 1  1 !  63
127 128 129 1  1 !  64
129 130 131 1  1 !  65
131 132 133 1  1 !  66
133 134 135 1  1 !  67
135 136 137 1  1 !  68
137 138 139 1  1 !  69
139 140 141 1  1 !  70
141 142 143 1  1 !  71
143 144 145 1  1 0.0 0.0 -0.3125 0.0 !  72 these elements with load on in y
dir
145 146 147 1  1 0.0 0.0 -0.3125 0.0 !  73
147 148 149 1  1 0.0 0.0 -0.3125 0.0 !  74
149 150 151 1  1 0.0 0.0 -0.3125 0.0 !  75
151 152 153 1  1 0.0 0.0 -0.3125 0.0 !  76
153 154 155 1  1 0.0 0.0 -0.3125 0.0 !  77
155 156 157 1  1 0.0 0.0 -0.3125 0.0 !  78
157 158 159 1  1 0.0 0.0 -0.3125 0.0 !  79
159 160 161 1  1 !  80
161 162 163 1  1 !  81
163 164 165 1  1 !  82
165 166 167 1  1 !  83
167 168 169 1  1 !  84
169 170 171 1  1 !  85
171 172 173 1  1 !  86
173 174 175 1  1 !  87
175 176 177 1  1 !  88
177 178 179 1  1 !  89
179 180 181 1  1 !  90
181 182 183 1  1 !  91
183 184 185 1  1 !  92
185 186 187 1  1 !  93
187 188 189 1  1 !  94
189 190 191 1  1 !  95
191 192 193 1  1 !  96
193 194 195 1  1 !  97
195 196 197 1  1 !  98
197 198 199 1  1 !  99
199 200 201 1  1 ! 100
*internal solution points
 10   -.5
 10.  -1.
 10.  -1.5
 10.  -2.
 *end
```

APPENDIX C - COMPILING PROGRAMS AND SETTING DATA STRUCTURE SIZES

The main BE program is called *gbed4* and is written in FORTRAN 77 with few non-standard extensions being used. It is compiled from the following source code files. No external subroutine packages are used.

gbed4.for - contains the main program
be_dim.inc - sets parameters for array dimensions (see below)
be_subs.inc - contains lower level routines for setting up and solving the BE matrices
io_subs.for - contains routine used in the input routines
gb_inp.inc - contains data input routines

The following files are used to compile the program *gb4chk* which is called by the Matlab program *beplot* for checking the data. Note that it uses the same input routines file, and array dimension parameters, include files as *gbed4* so that any changes to the data reading routines or error messaged generated by the main program will automatically be included in this program when it is recompiled.

gb4chk.for - main program
be_dim.inc - sets parameters for array dimensions (see below)
io_subs.for - contains routine used in the input routines
gb_inp.inc - contains data input routines

The following files are used to compile the utility program, *ex_frf*, for extracting frequency response function data from the output file of *gbed4*.

ex_frf.for - main program
fileread.for - file reading subroutines.

The Fortran include file *be_dim.inc* is listed below. The comments in this file indicate the meaning of the parameters that are set for dimensioning the arrays within the program. These should be set with regard to the mesh sizes required and the memory available on the computer.

```
c       fortran include file to be compiled with gbed4.for
c       cjcj 18-9-98
c
c       Sets array dimension parameters at top of each subroutine in gbed4
c
C       Set array declaration sizes
C       nne= Maximum number of elements
C       nx=  Maximum number of degrees of freedom = 2* number of nodes
C       nx=  2*Maximum number of nodes= 4*Maximum number of elements
C       nx1= 3*Maximum number of nodes= 6*Maximum number of elements
C       npm=Maximum number of field points
C       nfm=Maximum number of frequencies
C
      integer nne,nx,nx1,npm,nfm
      parameter(nne=300,nx=1200,nx1=1800,npm=1600,nfm=200)
```